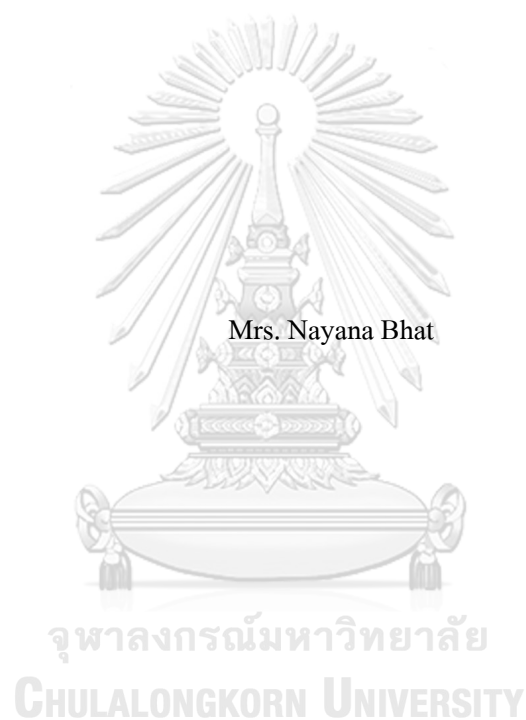


SUBSTRATE BINDING MECHANISM OF GLYCEROPHOSPHODIESTERASE TOWARDS
PESTICIDES AND IMPROVEMENT OF STABILITY BY MUTATIONAL ANALYSIS



A Dissertation Submitted in Partial Fulfillment of the Requirements
for the Degree of Doctor of Philosophy in Biochemistry and Molecular Biology

Department of Biochemistry

FACULTY OF SCIENCE

Chulalongkorn University

Academic Year 2021

Copyright of Chulalongkorn University

กลไกการยึดจับสารตั้งต้นของกลีเซอโรฟอสโฟไดเอสเทอร์สกับสารฆ่าแมลงและการปรับปรุง
ความเสถียร โดยการวิเคราะห์การกลายพันธุ์



วิทยานิพนธ์นี้เป็นส่วนหนึ่งของการศึกษาตามหลักสูตรปริญญาวิทยาศาสตรดุษฎีบัณฑิต
สาขาวิชาชีวเคมีและชีววิทยาโมเลกุล ภาควิชาชีวเคมี
คณะวิทยาศาสตร์ จุฬาลงกรณ์มหาวิทยาลัย
ปีการศึกษา 2564
ลิขสิทธิ์ของจุฬาลงกรณ์มหาวิทยาลัย

นยนา ภัท : กลไกการยึดจับสารตั้งต้นของกลีเซอโรฟอสโฟไดเอสเทอเรสกับสารฆ่าแมลงและการปรับปรุงความเสถียรโดยการวิเคราะห์การกลายพันธุ์. (SUBSTRATE BINDING MECHANISM OF GLYCEROPHOSPHODIESTERASE TOWARDS PESTICIDES AND IMPROVEMENT OF STABILITY BY MUTATIONAL ANALYSIS) อ.ที่ปรึกษาหลัก : ชาญญดา รุ่งโรจน์มงคล, อ.ที่ปรึกษาร่วม : อลิสา วังโน



สาขาวิชา	ชีวเคมีและชีววิทยาโมเลกุล	ลายมือชื่อนิสิต
ปีการศึกษา	2564	ลายมือชื่อ อ.ที่ปรึกษาหลัก
		ลายมือชื่อ อ.ที่ปรึกษาร่วม

5972824923 : MAJOR BIOCHEMISTRY AND MOLECULAR BIOLOGY

KEYWORD: Molecular dynamics bioremediation organophosphate pesticides inhibition kinetics

Glycerophosphodiesterase methyl parathion hydrolase

Nayana Bhat : SUBSTRATE BINDING MECHANISM OF GLYCEROPHOSPHODIESTERASE TOWARDS PESTICIDES AND IMPROVEMENT OF STABILITY BY MUTATIONAL ANALYSIS. Advisor: Assoc. Prof. THANYADA RUNGROTMONGKOL, Ph.D Co-advisor: Prof. ALISA VANGNAI

Molecular dynamics studies have been providing a great number of atomistic details of biological systems to understand enzymatic activity and underlying reaction mechanisms. Herein, molecular dynamic (MD) simulations were employed to study the binding mechanisms of organophosphate pesticides towards two metallohydrolases, i.e., glycerophosphodiesterase (GpdQ) and methyl parathion hydrolase (MPH). OPH are the class of enzymes which breaks down harmful organophosphates, including the pesticides and warfare agents into less harmful byproducts. Hence, these enzymes are excellent candidates for bioremediation. In the present study, various nonspecific organophosphate pesticides were docked into GpdQ and MPH enzymes to construct the pesticide/protein complex for performing MD simulations for 500 ns. In the first part, profenofos, chlorpyrifos and diazinon in complex with GpdQ were carried out. From MD results, all three were well stabilized by the active site and the residues P228, Q166, M167, I170, Y230. However, the distance between the metal ions was increased to accommodate the bulkier substrates. In part II, methyl paraxon, dichlorvos and profenofos binding to the cobalt and zinc bound MPH enzyme were studied. It was observed that methyl paraxon and dichlorvos favored cobalt bound MPH, whereas the profenofos had better binding free affinity towards zinc bound MPH. All pesticides coordinated with beta metal ion with a distance of 1.90 – 1.98 Å. In part III, the inhibition activity of cobalt bound MPH by carbamates such as carbofuran and carbaryl was investigated by *in vitro* and *in silico* studies. Enzyme kinetics study and Lineweaver-Burk plots exhibited uncompetitive inhibition for both carbamates. The molecular docking and MD simulations showed that among three possible binding sites, both carbamates preferred to bind at the groove between the two chains. The residues A260, P322 and L303 stabilized through π -alkyl interactions and H-bonds with S87, R319, and F320 were formed. This study has provided promising results of effective use of the organophosphate hydrolases in bioremediation.

Field of Study:	Biochemistry and Molecular Biology	Student's Signature
Academic Year:	2021	Advisor's Signature
		Co-advisor's Signature

ACKNOWLEDGEMENTS

First and foremost, I would like to extend my heartfelt gratitude to my supervisor I would like to thank my advisor, Assistant Professor Dr. Thanyada Rungrotmongkol as well as my Co advisor Professor Dr. Alisa Vangnai for helping me develop a solid understanding and passion for application of computational biology in bioremediation. Thank you for being very patient and providing creative ideas and suggestions that enlightened me all through my Ph.D. journey.

I would like to extend my gratitude to the chairman Associate Professor Dr. Supaart Sirikantaramas. My sincere thanks to Assistant Professor Dr. Rath Pichyangkura, Dr. Kittikhun Wangkanont, Professor Dr. Supot Hannongbua and Assistant Professor Dr. Nadtanet Nunthaboot for being on my committee and providing valuable advice.

I am deeply indebted to Dr. Bodee Nutho for sharing his time and expertise throughout my research. I would also express my appreciation to Mr. Jittakorn Thongnan for extending his help in the lab.

I would also like to thank the staff members and all my friends from the Department of Biochemistry, Faculty of Science, Chulalongkorn University for providing helping hand and making my time in the department memorable. My sincere thanks are expressed to all members of Biosim Lab, and Environmental biotechnology research unit lab members, from the Department of Biochemistry, Chulalongkorn University for their helpful encouragement and inspiration.

This research is supported by the 90th Anniversary of Chulalongkorn University Fund (Ratchadaphiseksomphot Endowment Fund).

Finally, I would like to express my deepest gratitude and appreciation to my parents, husband and my daughter for their encouragement, infinite love, and their untiring and constant support during this period.

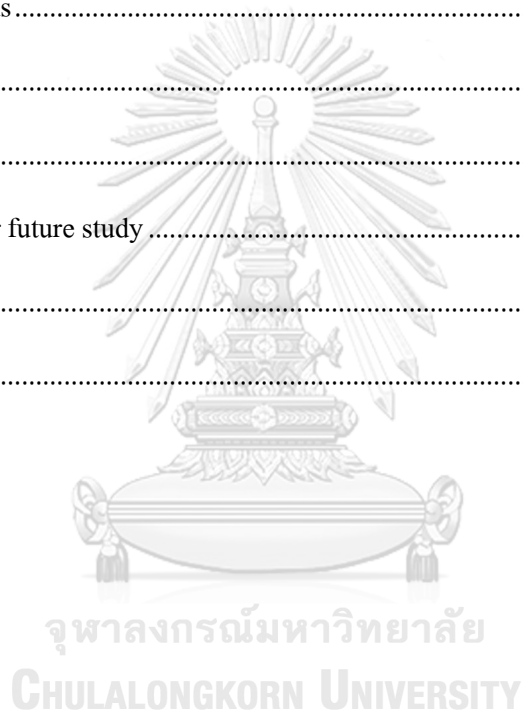
Nayana Bhat

TABLE OF CONTENTS

	Page
.....	iii
ABSTRACT (THAI).....	iii
.....	iv
ABSTRACT (ENGLISH).....	iv
ACKNOWLEDGEMENTS.....	v
TABLE OF CONTENTS.....	vi
LIST OF PUBLICATION.....	1
INTRODUCTION.....	2
1.1 Research concept.....	2
1.2 Research rationality.....	2
1.3 Research objectives.....	5
1.4 Expected beneficial outcome(s) from the thesis.....	5
Chapter 1.....	6
Manuscript 1.....	6
1. Introduction.....	8
2. Computational Methods.....	12
2.1 System preparation and Molecular Docking.....	12
2.2 Molecular dynamics (MD) simulations.....	14
2.3 Binding free energy calculation based on the MM/GBSA method.....	15
3. Results and Discussion.....	16
3.1 Binding affinity and key binding residues.....	24

4. Conclusion	27
Declaration of competing interest	28
Funding	28
Chapter 2	29
Manuscript 2.....	29
1. Introduction.....	31
2. Computational Methods.....	35
2.1 System preparation and Molecular Docking	35
2.2 Molecular dynamics (MD) simulations	37
3. Results and discussion	38
3.1 Substrate binding	38
3.2 Binding affinity and key binding residues	42
Conclusion	44
Chapter 3	46
Manuscript 3.....	46
1. Introduction.....	48
2. Materials and methods	50
2.1. Chemicals and reagents	50
2.2. Enzyme activity assay.....	50
2.3. Kinetics of inhibition of MPH by carbamates	51
2.4. Prediction of ligand binding site.....	51
2.5. Molecular docking of carbamates.....	52
2.6. Molecular dynamics simulations of carbamates/MPH complexes	52
2.5. Statistical analysis	53

3. Results.....	54
3.1 Enzyme kinetics	54
3.2 Ligand binding site prediction	55
3.3 Molecular docking	56
3.4 Molecular dynamics simulations	58
3.4 Interaction analysis	61
4. Conclusions.....	63
CONCLUSIONS.....	66
3.1 Conclusions	66
3.2 Suggestion for future study	67
REFERENCES	68
VITA	79



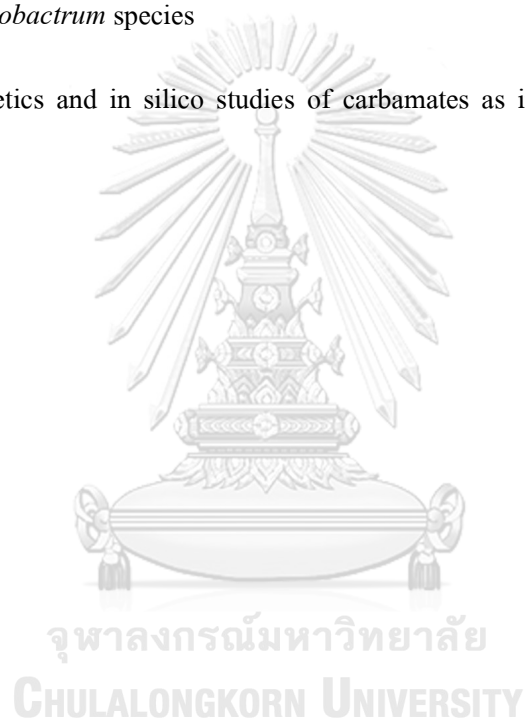
LIST OF PUBLICATION

This thesis contains general summary (introduction, some background information and conclusion) and the following paper which are referred to in the text by their roman number.

Manuscript I: Substrate binding mechanism of glycerophosphodiesterase towards organophosphate pesticides

Manuscript II: Molecular binding of a different classes of organophosphates to methyl parathion hydrolase from *Ochrobactrum* species

Manuscript III: Kinetics and in silico studies of carbamates as inhibitors of methyl parathion hydrolase



INTRODUCTION

1.1 Research concept

This research aimed to understand substrate binding mechanisms of glycerophosphodiesterase (GpdQ) and methyl parathion hydrolase (MPH) and their role in bioremediation of organophosphate pesticides. Different classes of organophosphate pesticides were docked into the active site of two metallohydrolase enzyme. The molecular dynamics simulations were performed to investigate the binding mechanism of the pesticides, their structural and dynamic properties of the enzyme. Finally, the synergism of the methyl parathion hydrolase enzyme was studied with two different carbamate pesticides. The inhibition kinetics was studied spectroscopically, and the binding site of the inhibitor was determined by molecular dynamic simulations. These findings suggest that the metallohydrolase enzyme can be successfully used for bioremediation of the pesticides. (All manuscripts as part of the thesis for graduation)

1.2 Research rationality

Organophosphates (OP) find many applications as plasticizers, lubricants, fuel additives, chemical warfare agents and pesticides since industrial revolution in mid-1940's.¹⁻² OP pesticides account for total of 38% of global pesticide consumption.³ They are also over exploited in agriculture consequently leading to environmental pollution. These chemicals also have significant adverse effects in animals and also in non-target species including humans because of their acetylcholinesterase inhibitory activity that have a profound effect on the nervous system.⁴⁻⁵

The worldwide health problem of acute pesticide poisoning is of 200,000 death annually.⁶ Many organophosphate pesticides such as profenofos, dichlorvos, chlorpyrifos and diazinon are still excessively used all over the world in spite of its harmful effects. To overcome environmental hazard, “green and clean” approach is required to degrade these pesticides. Certain enzymes are known to hydrolyze these OP compounds into less harmful byproducts have already been discovered in many microorganisms. These enzymes include phosphotriesterase (PTE)⁷⁻⁸ organophosphorus hydrolases (OPHs),^{7, 9-13} serum paraoxonase (PONs),¹⁴⁻¹⁶ methyl parathion hydrolases (MPHs),¹⁷⁻²¹ diisopropylfluorophosphate fluorohydrolase (DFPase),²¹⁻²² organophosphate acid anhydrolases (OPAAAs),²³⁻²⁴ glycerophosphodiesterase (GpdQ)²⁵⁻²⁹ and phosphotriesterase-Like-Lactonases (PLLs).³⁰⁻³⁶

Of these different metallohydrolases glycerophosphodiesterase and methyl parathion hydrolase has caught recent attention due to large substrate range and its ability to breakdown the substrate at broad range of pH and in presence of metal ions. Glycerophosphodiesterase (GDPDs; EC 3.1.4.46) are the enzymes that catalyzes the hydrolysis of the 3'-5' phosphodiester bond of glycerophosphodiesters. The glycerophosphodiesterase (GpdQ) from *Enterobacter aerogenes* has gained popularity as it not only degrades its natural substrate glycerol-phosphoethanolamine but also broad range of substrates such as phosphomonoester, phosphotriester and phosphorothiolate. The enzyme is seen to have a large pH range. More interestingly, the GpdQ finds its application in breaking down of toxic phosphodiesters. Whereas methyl paraoxon hydrolases (MPHs) are coded by *mpd* (methyl parathion degradation) genes. They are known to hydrolyze methyl

parathion. They are aryldialkylphosphatases with conserved metallo- β -lactamase domains. The *mpd* genes were first identified in *Plesiomonas* sp. strain M6 and were later discovered in bacterial species such as *Achromobacter*, *Ochrobactrum*, *Stenotrophomonas* and *Pseudomonas*.^{18,}
^{20, 37-38} The *mpd* genes do not share sequence homology with other OP-degrading genes.

In this thesis, we address the applications of these metallohydrolases in breakdown of organophosphate pesticides using computational approach. Through modelling and computational simulations, the atomistic world of the active site of the enzyme can be explored. It also gives insights on the interactions and the forces that act upon the breaking down of the substrate. The role of metal ions, substrate specificity and binding mechanism in the two metallohydrolase enzyme i.e., glycerophosphodiesterase and methyl parathion hydrolase is well studied in this work. Apart from that the synergistic/inhibitory activity of the carbamates towards the methyl parathion hydrolase enzyme is studied both computational approach and inhibition kinetics. This would give better understanding of binding cavities of the enzyme and its interacting amino acid residues.

The thesis is briefly divided into three chapters corresponding to three manuscripts. The first chapter provides computational studies of binding three organophosphate pesticides i.e., profenofos, chlorpyrifos and diazinon to glycerophosphodiesterase enzyme. The second chapter explores the application of methyl parathion hydrolase enzyme as bioremediator for organophosphate pesticides such as profenofos and dichlorvos. The metal ion promiscuity (zinc and cobalt) of the enzyme with the organophosphates pesticides as substrate is also explored. In

the third chapter the inhibition and other binding sites of the methyl parathion hydrolase enzyme are studied by kinetics and computational approach respectively. Conclusions and future work and limitations are addressed in the last chapter.

1.3 Research objectives

1. To understand the binding mechanism of the glycerophosphodiesterase and methyl parathion hydrolase towards organophosphate pesticides.
2. To compare the stability and activity of methyl parathion hydrolase with different metal ions such as zinc and cobalt
3. To study the synergism of the methyl parathion hydrolase towards carbamates such as carbofuran and carbaryl

1.4 Expected beneficial outcome(s) from the thesis

This study helps us in understanding the functioning of metallohydrolase enzymes in breaking down of real scenario substrates as opposed to its natural substrates. Thus, helping in rational design of environmentally friendly bioremediation agents to these harmful pesticides.

Chapter 1

Manuscript 1

Substrate binding mechanism of glycerophosphodiesterase towards organophosphate pesticides

Nayana Bhat¹, Bodee Nutho², Alisa Vangnai^{1,3}, Kaito Takahashi⁴, Thanyada Rungrotmongkol^{1,5*}

¹*Biocatalyst and Environmental Biotechnology Research Unit, Department of Biochemistry, Faculty of Science, Chulalongkorn University, Bangkok 10330, Thailand*

²*Center of Excellence in Computational Chemistry (CECC), Department of Chemistry, Faculty of Science, Chulalongkorn University, Bangkok 10330, Thailand*

³*Center of Excellence in Hazardous Substance Management, Chulalongkorn University, Bangkok 10330, Thailand*

⁴*Institute of Atomic and Molecular Sciences, Academia Sinica, Taipei-10617, Taiwan*

⁵*Program in Bioinformatics and Computational Biology, Graduate School, Chulalongkorn University, Bangkok 10330, Thailand*

*Corresponding author. Email: thanyada.r@chula.ac.th, t.rungrotmongkol@gmail.com

Phone: +66-2218-5426. Fax: +66-2218-5418.

จุฬาลงกรณ์มหาวิทยาลัย
CHULALONGKORN UNIVERSITY

Accepted manuscript in journal of molecular liquids

<https://doi.org/10.1016/j.molliq.2021.115526>

Substrate binding mechanism of glycerophosphodiesterase towards organophosphate pesticides

Nayana Bhat¹, Bodee Nutho², Alisa Vangnai^{1,3}, Kaito Takahashi⁴, Thanyada Rungrotmongkol^{1,5*}

¹*Biocatalyst and Environmental Biotechnology Research Unit, Department of Biochemistry, Faculty of Science, Chulalongkorn University, Bangkok 10330, Thailand*

²*Center of Excellence in Computational Chemistry (CECC), Department of Chemistry, Faculty of Science, Chulalongkorn University, Bangkok 10330, Thailand*

³*Center of Excellence in Hazardous Substance Management, Chulalongkorn University, Bangkok 10330, Thailand*

⁴*Institute of Atomic and Molecular Sciences, Academia Sinica, Taipei-10617, Taiwan*

⁵*Program in Bioinformatics and Computational Biology, Graduate School, Chulalongkorn University, Bangkok 10330, Thailand*

*Corresponding author. Email: thanyada.r@chula.ac.th, t.rungrotmongkol@gmail.com

Phone: +66-2218-5426. Fax: +66-2218-5418.

Abstract:

Glycerophosphodiesterase (GpdQ) from *Enterobacter aerogenes* is a binuclear metallohydrolase, which is capable of catalyzing the hydrolysis of mono-, di-, and tri-ester substrates, including some organophosphate pesticides and degradation products of nerve agents. The GpdQ has attracted recent attention as a promising enzyme for bioremediation. This enzyme

utilizes two metal ions located in the α and β sites of the enzyme active site for catalysis and is found to bind to Fe(II) ion preferentially. In this study, we aimed to investigate the binding interactions of three organophosphate pesticides (i.e., profenofos, diazinon and chlorpyrifos) to the GpdQ using computational approaches. Firstly, each pesticide molecule was separately docked into the active site of the GpdQ using molecular docking. Then, 500-ns MD simulations were carried out on the systems without (apo enzyme) and with pesticides bound. The MD results showed that the Fe β binds well with the GpdQ active site in the presence of pesticide. It is also seen that the binding of the pesticide could stabilize the enzyme structure in the active conformation, allowing the substrate to be catalysed into less harmful products. Therefore, the ability of *in silico* analysis presented here could be informative for enhancing enzyme stability and activity in the future.

Keyword: glycerophosphodiesterase; organophosphate pesticides; computational simulations

1. Introduction

Glycerophosphodiesterases (GpdQ, EC 3.1.4.46) is the class of enzymes that catalyze the hydrolysis of the 3'-5' phosphodiester bond of glycerophosphodiester.³⁹⁻⁴⁰ Specifically, GpdQ from *Enterobacter aerogenes* has gained popularity as it can degrade its natural substrate glycerol-phosphoethanolamine⁴¹ and a broad range of substrates such as phosphomonoester, phosphotriester and phosphorothiolate at a large pH spectrum.^{25, 42-43} More interestingly, the GpdQ can be used in the breaking down of toxic phosphodiester.⁴⁴ This came to attention in the 1970s when Gerlt and co-workers purified GpdQ and investigated its function.⁴² Since the GpdQ rapidly degrades some organophosphates (OPs), it has been used as an effective bioremediator to

eliminate harmful nerve agents and pesticides such as profenofos, diazinon, and chlorpyrifos and so on.^{26, 45-46}

The GpdQ is a metallohydrolase containing two metal ions (α and β metal ions) at the enzyme active site, which can also be presented either as homo or hetero dimer. However, the metal ion content of the GpdQ *in vivo* is currently unknown and may be present as homonuclear (Zn, Mn, Ni, etc.) or heteronuclear forms.^{40, 47} Based on spectroscopic and crystallographic results, it was initially proposed that the native metal ion composition was Fe(II) and Zn(II) ions.²⁷ Nonetheless, the reactivity of apo-GpdQ has been readily reconstituted with Co(II), Mn(II), Fe(II), Zn(II) and even Cd(II).^{27, 29, 43, 48} Anomalous scattering experiments also demonstrated that Fe(II) ion was likely to be preferred at the α site.²⁶

To date, the X-ray crystal structures of dimeric GpdQ with different metal ions (Co, Zn, and Fe) bound are available in the Protein Data Bank (PDB accession codes 2DXL⁴⁸, 2DXN⁴⁸ and 2ZO9²⁸, respectively). In addition, mutagenesis study suggested that β metal affinity can be increased by replacing the residue N80 with aspartate (N80D).²⁷ However, the catalytic activity is greatly compromised. Further investigation revealed that the occupancy of the metal ion is 0.75 and 0.45 for the α and β sites, respectively.²⁸ This implied that the metal ion at the α site is bound more tightly than that in the β site, and consequently the GpdQ is predominantly presented as a mononuclear enzyme in the resting state.^{25-26, 49} In the presence of a natural substrate, the metal ion affinity of the β site was increased, which led to the formation of a catalytically competent binuclear active site.²⁶⁻²⁸ Subsequently, the coordination between the

metal ion in the β site and N80 is broken upon substrate binding. A terminal hydroxide then acts as a nucleophile, resulting in the release of the product and the β metal ion. As a result, the enzyme active site returns to its mononuclear resting state.²⁸ Additionally, a water molecule binds to the active site, which acts as nucleophilic donor for catalysis.^{26, 40} Note that the α -coordination sphere consists of the residues H10, H197 and D50 as equatorial ligand and D8 as an axial ligand. In contrast, the β -site coordination sphere comprises the residues H195, N80 and D50 as equatorial ligands and H156 as an axial ligand (Figure 1B). The residue N80 is also found to play an important role in regulating enzymatic activity.²⁶ In addition to these residues, Y19, H81 and H217 is known to play role catalysis. Specifically, H217 acts as catalytic acid/base residue.⁵⁰

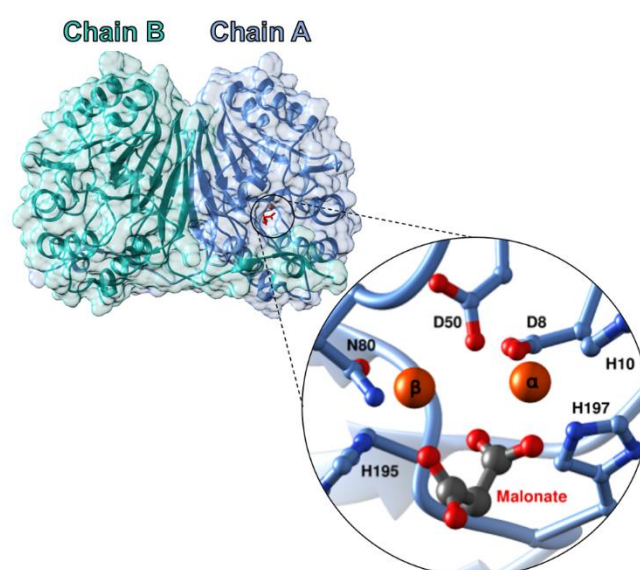


Figure 1. X-ray crystal structure of the GpdQ in complex with malonate substrate (PDB ID: 2Z09). Chain A and chain B of the GpdQ are shaded by blue and green colors, respectively. The close-up region of malonate-bound substrate binding pocket, as well as Fe metal ions at the α and β sites coordinating with the active site residues is also shown.

OPs are a class of pesticide that is widely used in agriculture, and nearly 40% of the contributed are OPs.⁵¹ OPs are toxic compounds as they can irreversibly inhibit acetylcholinesterase,⁵² which is an enzyme involved in neurotransmission. These compounds are also mutagenic, leading to nervous and immune system-related diseases.⁵³⁻⁵⁵ Moreover, OPs commonly contaminate water and soil due to their partial soluble nature. Occupational exposure or environmental contamination causes poisoning. When OPs are dumped into landfills, they leach into soil and decompose to produce toxic substances.⁵⁶ To overcome this environmental hazard, there should be a “green and clean” approach.⁵⁷ One of the most powerful strategies is to use a microorganism that has special enzymes to degrade these harsh chemicals. The OP-degrading enzymes have been studied since 1946. The enzyme was discovered in mammalian tissue extracts, and fortunately the hydrolysis of diisopropylfluorophosphate (DFP) was observed.⁵⁸ Later in 1973, it was seen that the soil bacterium *Flavobacterium sp.* (strain ATCC 27551) was capable of hydrolyzing the OP diazinon.⁷ *Agrobacterium radiobacter*, *Enterobacter aerogenes* and *Pseudomonas diminuta* were also known to have enzymes that degrade several OPs.^{39, 45-46, 59}

In silico analysis of the GpdQ would be useful to improve the activity and stability of the enzyme, particularly the OPs-degrading enzymes. Three pesticides, namely profenofos, diazinon and chlorpyrifos are focused in this study (**Figure 2**) as they are the pesticides that are known to be harmful and banned in many countries but still prevalent in nature and used in developing nations. We aimed to obtain basic information for improvement of GpdQ to degrade OPs by investigating the binding of three organophosphate pesticides. Molecular docking was carried out in the

substrate-binding pocket of the GpdQ in order to investigate the binding mode of these OP pesticides, in which the two Fe(II) metal ions were occupied in the α and β sites.⁶⁰ After that, the best pose obtained from molecular docking was chosen, and MD simulations were conducted on the systems of the OP pesticides in complex with the GpdQ. The acquired information would provide detailed insight into the mechanism of the OPs binding and characteristic of the metal ion against the GpdQ. We also investigate how the binding situation varies when we change from small substrate mimics to real pesticides.

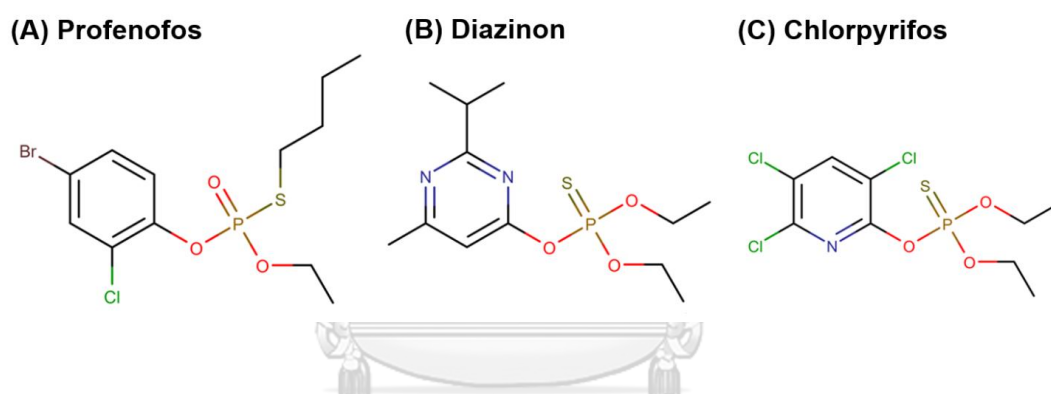


Figure 2. Chemical structures of three OP pesticides: (A) profenofos (B) diazinon and (C) chlorpyrifos.

2. Computational Methods

2.1 System preparation and Molecular Docking

The initial X-ray structure with 2.2 Å resolution of GpdQ with Fe(II) bound and in complex with malonate was obtained from the PDB, accession code 2ZO9.²⁸ The protonation states of all ionizable amino acids (D, E, K, R and H) were assigned at pH 7.0 using PROPKA3.1.⁶¹ Their environments were also visually explored by considering the possibility of

hydrogen bonding with the surrounding residues. The AMBER ff14SB force field was applied for the protein.⁶² The three OP pesticides profenofos, diazinon and chlorpyrifos were built using the Gaussview5.0 program. Consequently, the electrostatic potential (ESP) charges of each ligand were computed by HF/6-31G(d) level of theory using Gaussian09 program.⁶³ The restrained ESP (RESP) charges were obtained by converting the ESP charges using the antechamber module implemented in AMBER16. The atom types and the other molecular parameters of ligand were assigned by the general AMBER force field (GAFF)⁶⁴ using the parmchk program. The three OP pesticides were docked with 100 independent runs into the active site of the GpdQ using CDOCKER module⁶⁵ in the Accelrys Discovery Studio 2.5^{Accelrys Inc.}. It is to be noted that the malonate-bound position was defined as the binding site for the docking process. The suitable docked conformers of the GpdQ with each pesticide molecule were selected for subsequent molecular dynamics (MD) simulation. Afterward, the missing hydrogen atoms were added using the LeaP module of AMBER16. Each system was then solvated by TIP3P⁶⁶ water model in an octahedral box within 10 Å from protein surface with the box dimension of $109 \times 109 \times 109 \text{ \AA}^3$, approximately 17000 water molecules. Moreover, sodium counter ions were added to neutralize the system. To diminish the unfavourable contacts and steric hindrances, the solvent and counter ions were initially minimized by 1500 steps of steepest descent (SD) and 3000 steps of conjugate gradient (CG) methods, while the other molecules were restrained using a force constant of 500 kcal/mol·Å². After that, the protein was minimized by SD (1000 steps) and CG (2500 steps)

methods with a constrained solvent. Finally, the SD (1000 steps) and CG (2500 steps) minimizations were fully applied to the whole system.

2.2 Molecular dynamics (MD) simulations

MD simulations were simulated based on the standard procedure⁶⁷ using isothermal–isobaric ensemble (*NPT*) at a constant pressure of 1 atm equilibrated at 303 K⁴³ for 500 ns. The calculated simulation time step was set to 2 fs under periodic boundary condition. All covalent bonds involving hydrogen atoms were constrained using the SHAKE algorithm.⁶⁸ The particle-mesh of Ewald’s summation method⁶⁷ was used for the treatment of the long-range electrostatic interactions with 10 Å cut-off distance. Temperature and pressure were controlled by the Langevin dynamics⁶⁹ and Berendsen barostat⁷⁰, respectively. It is worth noting that each MD simulation of GpdQ–ligand complexes was performed by the AMBER16 software package coupled with the PMEMD module.⁷¹ The trajectories were collected for every 10 ps. The calculation of root-mean square deviation (RMSD) was applied to detect the system stability. RMSD of all atoms of the individual chain of GpdQ (chain A and chain B) and the pesticide was plotted along simulation time, as shown in **Supplementary Figure 1**. It was found that the RMSD values rapidly increased at the first 5 ns and slightly fluctuated until reaching 50 ns in all systems. All the GpdQ–pesticide complexes tended to be stable after 50 ns of MD simulation. Hence, the MD trajectories extracted from the last 50 ns (450–500 ns) of MD simulations were

considered for further analysis. Note that the relevant structural analyses were examined using the CPPTRAJ module of AMBER16.⁷²

2.3 Binding free energy calculation based on the MM/GBSA method

The molecular mechanics/generalized Born surface area (MM/GBSA) approach⁷³ was generally used to calculate the binding free energy (ΔG_{bind}) of the protein–ligand complex, which is computed by the free energy difference between the protein–ligand complex (G_{complex}) and its isolated forms (G_{protein} and G_{ligand}), as shown in Equation 1:

$$\Delta G_{\text{bind}} = G_{\text{complex}} - (G_{\text{protein}} + G_{\text{ligand}}) \quad (1)$$

The ΔG_{bind} consists of the molecular mechanical (MM) energy in gas phase (ΔE_{MM}), solvation free energy (ΔG_{solv}), and entropic contribution term ($T\Delta S$), as given in Equation 2:

$$\Delta G_{\text{bind}} = \Delta E_{\text{MM}} + \Delta G_{\text{solv}} - T\Delta S \quad (2)$$

The ΔE_{MM} is achieved from the combination of electrostatic (ΔE_{ele}) and van der Waal (ΔE_{vdw}) energies, whereas the ΔG_{solv} is calculated using Equation 3 below:

$$\Delta G_{\text{solv}} = \Delta G_{\text{solv}}^{\text{ele}} + \Delta G_{\text{solv}}^{\text{nonpolar}} \quad (3)$$

The $\Delta G_{\text{solv}}^{\text{ele}}$ can be estimated using the GB model⁷⁴, whereas the $\Delta G_{\text{solv}}^{\text{nonpolar}}$ is calculated using solvent accessible surface area (SASA)⁷⁵, as shown in Equation 4:

$$\Delta G_{\text{solv}}^{\text{nonpolar}} = \gamma \text{SASA} + b \quad (4)$$

where γ and b are the experimental solvation parameters equal to $0.00542 \text{ kcal/mol} \cdot \text{\AA}^2$ and 0.92 kcal/mol , respectively.⁷⁶ Additionally, the contribution of each amino acid residue involved in ligand binding was evaluated using the per-residue decomposition free energy ($\Delta G_{\text{bind}}^{\text{residue}}$) analysis.

3. Results and Discussion

The GpdQ is an oligomeric protein made up of trimer of dimeric subunits. These dimers are composed of identical subunits.⁴⁸ In this study, a dimer was used as an initial protein structure because it has been postulated that the active site is easily accessible when the enzyme is presented in the form of dimer rather than hexamer.⁴⁸ As noted in the introduction section, the GpdQ is a metalloenzyme coordinated with dinuclear metal center, the metal ion composition may vary based on natural abundance. Currently, many research have been conducted using various combinations of homo or heterodinuclear metal ions of Co, Mn, Fe, Cd and so on. However, in this study homodinuclear center with Fe(II) was chosen, as the previous report suggested that the enzyme is most likely to coordinate with at least one Fe metal ion.²⁸ Therefore, the crystal structure of the GpdQ, which had two Fe metals in the active site and bound with malonate, was used as the starting protein of interest (see method section). In this work, three OP pesticides, specifically two thiophosphotriester diazinon and chlorpyrifos and one *S*-substituted thiophosphotriester profenofos were docked into the substrate-binding site of the GpdQ using 100 docking runs. Note that the first carboxylate group of the native malonate coordinated in tridentate fashion with Fe_α (2.6 Å), Fe_β (2.4 Å) and H195 (2.7 Å). Whereas, the second

carboxylate group was coordinated with N80 (2.8 Å) and H81 (3.2 Å).²⁸ Based on these interactions, the docked conformers of each pesticide that had the similar binding pattern with malonate and exhibited the lowest CDOCKER interaction energy were presumed as the most possible binding mode and selected as the initial structures for subsequent MD simulation. It can be noticed from **Figure 3** that all pesticides profenofos (interaction energy of -45.37 kcal/mol), diazinon (-39.31 kcal/mol) and chlorpyrifos (-36.24 kcal/mol) gave the good interaction energies with the GpdQ. Hence, these docked structures were suitable for use as starting structures for MD simulation in the next step.

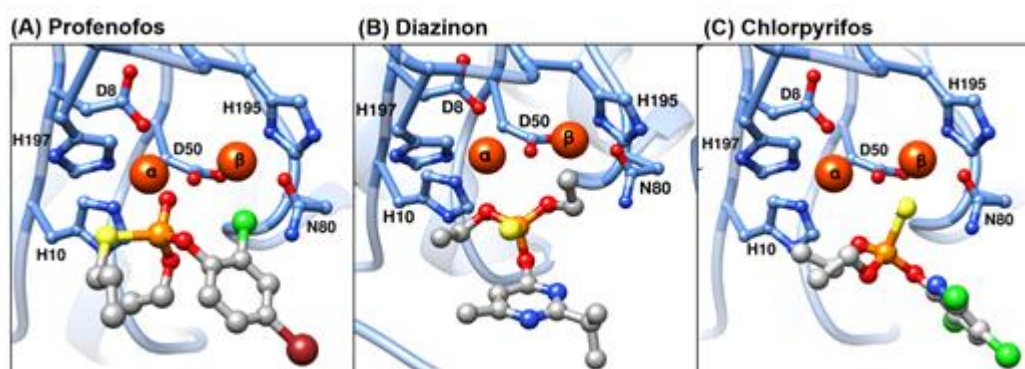


Figure 3. Docked structures of (A) profenofos, (B) diazinon and (C) chlorpyrifos binding to the GpdQ.

As mentioned previously, the GpdQ contains two metal ion sites accounting for its catalytic efficiency.^{27-28, 48} In fact, the α ion has higher occupancy and is tightly bound in comparison to the β ion.²⁶ In addition, the β ion binds only in the presence of a substrate.²⁷ Thus, the distance difference of the two metal ions can determine the stability of the enzyme active site upon pesticide binding. To monitor such distance along the simulation time, the distance between

the Fe_α and Fe_β ions was measured and depicted in **Figure 4**. The results showed that both Fe ions were found to be stable throughout the MD simulation in all the systems. Furthermore, the metal-metal distance was also dependent on the type of the bound ligand. In this regard, the Fe_α - Fe_β distance in each system was in the range of 4.5–5 Å which was much greater than the distance in the crystal structure (~3.5 Å). This is possibly due to the native structural chemistry of pesticides. Indeed, the GpdQ active site undergoes conformational changes including the distance of the metal ion pair to accommodate the bulkier pesticides to bind to the substrate-binding pocket. Hence, it is clearly seen that the binding of pesticides could affect the geometry of the GpdQ active site, particularly the Fe_α - Fe_β distance.

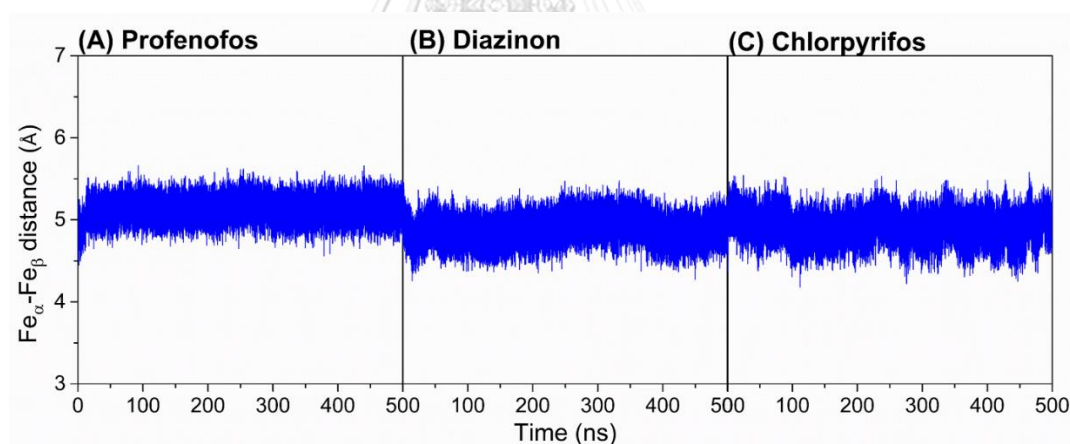


Figure 4. Distance between Fe_α and Fe_β ions located in the GpdQ active site in complex with (A) profenofos, (B) diazinon and (C) chlorpyrifos.

To understand the nature of the Fe_β ion upon pesticide binding, the structural superimposition were carried out over the 100 snapshots extracted from the last 50 ns of MD

simulation, compared to the crystal structure of the GpdQ complex (PDB code 2ZO9), as shown in **Figure 5**. As expected, the Fe_{α} position taken from MD snapshots was shown to be clustered, which was highly close to the Fe_{α} of the crystal structure. In contrast, the Fe_{β} position from each MD snapshot moved away from Fe_{β} of the crystal structure, which was consistent well with the lower occupancy of the β metal ion as supported from the experimental data.²⁸

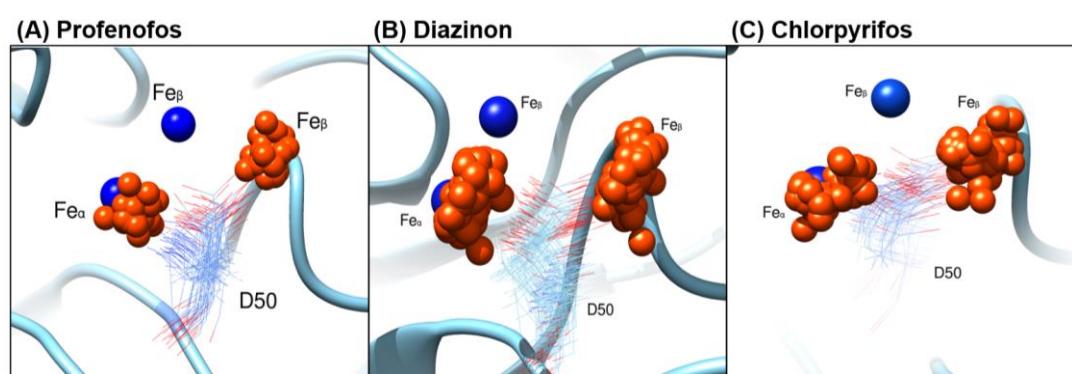


Figure 5. Overlay structures over the 100 snapshots of the GpdQ binding to (A) profenofos, (B) diazinon and (C) chlorpyrifos relative to the crystal structure. Both metal ions derived from the X-ray structure and MD snapshots are shown in blue and orange, respectively.

The active site structure of the GpdQ contains the binuclear metal center that is coordinated with the surrounding amino acids and the substrate.²⁷ Moreover, the preferential binding and coordination flexibility also depend on different substrates bound.⁷⁷ The amino acid residues in the GpdQ active site are mostly negatively charged, and the substrate is also negatively charged (e.g. malonate); thus, the substrate-binding pocket is necessarily stabilized by the positive charge of metal ions. With this information, the distance between each metal ion

(Fe α and Fe β) and the coordinating amino acids is given in Table 1 and depicted in Figure 6. Notably, the observation showed that the two metal ions were firmly coordinated with D50 in all the systems, as known as bridging residue (defined as Fe α ...D50...Fe β).²⁷ The coordination formations of all pesticides and surrounding residues with each metal ion are as follows: the OD1 atom of D50 was coordinated with the Fe β , while the OD2 atom was formed with the Fe α . The D50 switches position to interact with both the metal ions.⁷⁸ Note that the D50 stays almost at equidistance between the two ions (~ 1.90 Å) in all systems. Moreover, the Fe α coordinated with an additional residue D8 at a distance less than 2 Å. Apart from these two aspartate residues, the Fe α still coordinated with the NE2 atom of H10, which was thought to play a role in regulating the pH of the active site.²⁷ As noted, the Fe β metal ion has low occupancy and binds to the active site only in presence of the substrate binding.⁴⁰ In the apo form, D50 is predominantly bound to the Fe α , and the catalysis can take place when it binds to the Fe β .⁷⁸ Along with D50, the Fe β needed to coordinate with N80. This residue plays a significant role in the assembly of di-nuclear center and regulates enzymatic activity.²⁶ From our results, it is seen that upon pesticide binding the distance between N80 and Fe β ion reduces to the range of 2.00- 2.03 Å (as compared to 2.3 Å in the crystal structure). Due to change in the orientation of the active site, it is seen that the H195 did not coordinate with the moiety of chlorpyrifos and diazinon. In addition, all pesticides cannot coordinate with the Fe β ion unlike the natural substrate.⁷⁹ This reflected that different substrates employs different binding strategies.

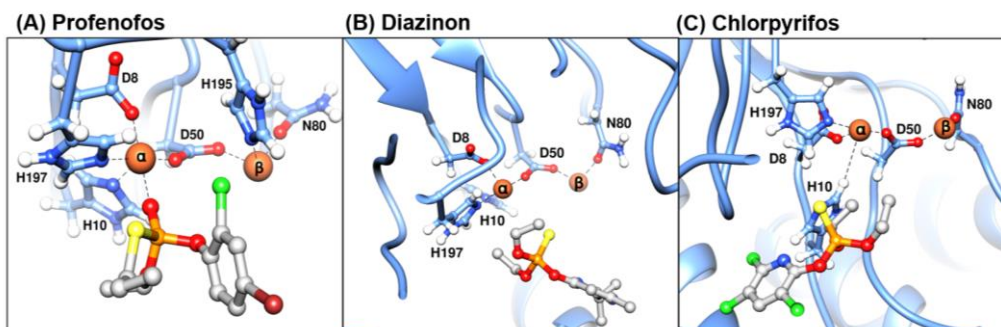


Figure 6. Coordination of Fe(II) with surrounding amino acids and each pesticide (coordination with water not shown): (A) profenofos, (B) diazinon and (C) chlorpyrifos.

Apart from the surrounding amino acids, the metal ion could also bind to the water molecule. It should be mentioned that the water molecule plays an important role as a nucleophilic donor in the catalysis and/or has a role in the substrate binding.²⁸ In this study, radial distribution function (RDF) is used to calculate the distance and number of water molecules around the Fe metal ions. The RDF is denoted $g(r)$ that represents the probability of finding a water molecule at a distance 'r' from the Fe metal ion. It was seen that Fe^{α} coordinated with one water molecule at a distance of 2.25 Å in profenofos system and two molecules of water in diazinon and chlorpyrifos systems (Supplementary Figure 2). Whereas the Fe^{β} ion was coordinated to oxygen atom of two water molecules at a distance of 2.25 Å in profenofos system and three molecules of water in diazinon and chlorpyrifos systems. However, for all pesticides, the coordination number of the Fe^{α} and Fe^{β} remains 6 and 4, respectively.

Table 1. Distance (Å) of the Fe α and Fe β with surrounding amino acids, pesticide, and water.

Fe-Alpha	D8_OD1	D50_OD2	H10_NE2	H197_NE2	Pesticide	Water
Profenofos	1.92 ± 0.05	1.92 ± 0.04	2.30 ± 0.12	2.16 ± 0.08	2.01 ± 0.06	2.25 (1)
Diazinon	1.90 ± 0.04	1.91 ± 0.04	2.37 ± 0.18	2.22 ± 0.11	7.30 ± 0.34	2.25 (2)
Chlorpyrifos	1.90 ± 0.04	1.92 ± 0.05	2.41 ± 0.51	2.27 ± 0.11	9.51 ± 2.50	2.25 (2)
Fe-Beta	D50_OD1	N80_OD1	H195_NE2	Pesticide	Water	
Profenofos	1.91 ± 0.04	2.00 ± 0.05	2.19 ± 0.10	5.77 ± 0.21	2.25 (2)	
Diazinon	1.93 ± 0.05	2.01 ± 0.06	4.56 ± 0.59	8.08 ± 0.69	2.25 (3)	
Chlorpyrifos	1.92 ± 0.04	2.02 ± 0.06	6.40 ± 0.38	11.43 ± 2.61	2.25 (3)	

The dynamics of pesticide system instead of substrate mimics highlights the importance of studying environmentally important substrates. The change in the binding strategies of the pesticides in comparison to malonate is seen as a change in the binding pocket size. As given in the **Figure 7.**, the active site of GpdQ adjusts its size by increasing the binding area to accommodate the bulky pesticide, and this flexibility of the enzyme is also important when searching for active enzymes targeted for bulk molecules.

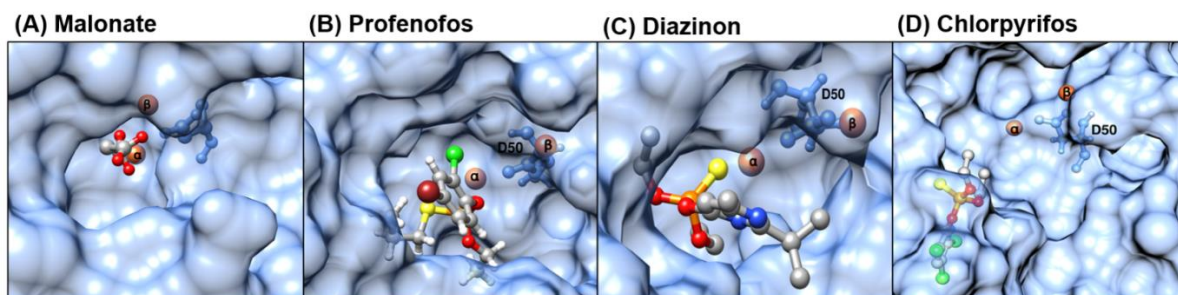


Figure 7. Volume of the active site bound to: (A) malonate, (B) profenofos, (C) diazinon and (D) chlorpyrifos.

The solvent accessible surface area (SASA) measures the fraction of the protein surface interacting with the solvent molecules. The area of active site was calculated on residues within a 4-Å sphere of each pesticide. For the pesticide systems the values ranged between 330 to 607 Å² for pesticide systems. Whereas the SASA value of malonate bound system (crystal structure) was just 56.06 Å². The SASA values are tabulated in **Table 2**. These observations indicate that the area of the active site is larger to accommodate the bulkier pesticides as compared to malonate (substrate mimic). Thus, MD simulations allows us to sample the various possible conformation of substrate binding.

Table 2. Average SASA of malonate and substrate bound systems.

	Average SASA (Å ²)
Malonate	58.06
Profenofos	330.38 ± 70.45
Diazinon	607.53 ± 87.19
Chlorpyrifos	603.88 ± 84.52

3.1 Binding affinity and key binding residues

The MM/GBSA method implemented in AMBER16 was used to estimate the binding free energies of the three different pesticides in complex with the GpdQ. The binding free energy of the complex is estimated from difference of free energy between the complex, protein and substrate (see method in more details). Normal mode analysis⁸⁰ in AMBER16 was done to calculate the entropy approximation which includes translational, rotational and vibrational contributions. In order to estimate the binding affinity of each pesticide towards the GpdQ, the MM/GBSA calculations were performed on 1000 snapshots from the last 50 ns. The energy components are tabulated in **Table 3**. From the interaction energy in gas phase (ΔE_{MM}), it is evident that profenofos has a better binding affinity as compared to the remaining systems. It was found that attractive coulombic interactions (ΔE_{ele}) were the stabilizing force for the profenofos binding, whereas the other two pesticides systems suggested that the van der Waals (ΔE_{vdw}) energy was the driving force for inducing molecular complexation. Furthermore, the polar ($\Delta G_{solv}^{ele} + \Delta E_{ele}$) and nonpolar ($\Delta G_{solv}^{nonpolar} + \Delta E_{vdw}$) contributions were also specified in **Table 3**. The results indicated that profenofos was stabilized by the polar interaction rather than the nonpolar energy contribution. In contrast, the energy contribution for binding of diazinon and chlorpyrifos to the GpdQ significantly came from the nonpolar term. Altogether, the binding free energy (ΔG_{bind}) including the entropic term of profenofos, diazinon and chlorpyrifos were -22.83 ± 3.40 , -13.38 ± 4.97 and -9.32 ± 1.63 kcal/mol, respectively, suggesting that profenofos had the stronger binding affinity against the GpdQ, compared with other two pesticides.

Table 3. The binding free energy and its energy components (kcal/mol) calculated with the MM/GBSA approach.

	Profenofos	Diazinon	Chlorpyrifos
ΔE_{ele}	-81.26 ± 4.42	-14.84 ± 2.84	-4.37 ± 5.30
ΔE_{vdW}	-28.73 ± 2.54	-35.52 ± 1.92	-32.44 ± 3.80
ΔE_{MM}	-109.99 ± 3.90	-50.37 ± 3.46	-36.81 ± 6.84
$\Delta G_{solv}^{nonpolar}$	-4.57 ± 0.13	-4.80 ± 0.19	-3.64 ± 0.387
ΔG_{solv}^{ele}	73.01 ± 3.29	28.38 ± 3.23	13.62 ± 5.60
ΔG_{sol}	68.42 ± 3.24	23.58 ± 3.28	9.98 ± 5.51
$\Delta G_{solv}^{nonpolar} + \Delta E_{vdW}$	-33.30 ± 2.54	-38.32 ± 1.92	-36.08 ± 3.80
$\Delta G_{solv}^{ele} + \Delta E_{ele}$	-8.25 ± 4.42	13.48 ± 2.84	9.25 ± 5.30
ΔG_{total}	-41.55 ± 0.07	-26.78 ± 2.06	-26.83 ± 3.59
$-T\Delta S$	18.73 ± 1.05	20.00 ± 4.09	17.50 ± 4.28
ΔG_{bind}	-22.83 ± 3.40	-13.38 ± 4.97	-9.32 ± 1.63

To pinpoint the key residues within the substrate-binding pocket involved in the binding of the GpdQ–ligand complexes, the per-residue decomposition free energy ($\Delta G_{bind}^{residue}$) calculation based on the MM/GBSA approach was performed. The energy contribution of each residue from chain A of the GpdQ towards each pesticide binding and the position of binding residues around the pesticide are represented in **Figure 8**. Most of the residues in the active site (i.e., D8, H10, D50, H195, H197) exhibited good energy stabilizations (negative values) with all pesticides in the range of -2.41–-0.23 kcal/mol. Apart from the chain A residues, Y263 located in the chain B (Y534) of the GpdQ was another important residue associated with pesticide binding.

This residue was seen to form π -alkyl interactions with each pesticide molecule (Figure 8, right). Besides, various second coordination shell residues such as Y19, Q166, M167, I170, V219, P228, Y230 were found to stably interact with the pesticide. These interactions were predominant *via* alkyl interactions and/or weak hydrogen bonds. Considering hydrogen bonding and the per-residue binding free energy decomposition, it was observed that there was good protein-metal ion and substrate interaction. Out of the 3 pesticides, it was clearly seen that the profenofos showed the better interactions towards the GpdQ as supported from the total binding free energy calculation mentioned above.

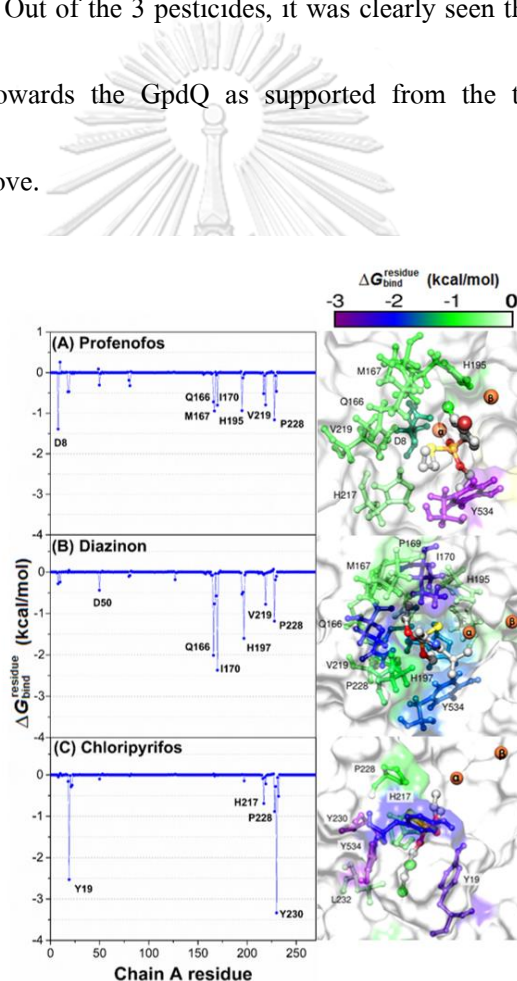


Figure 8. Per-residue decomposition free energy ($\Delta G_{\text{bind}}^{\text{residue}}$) on the systems of the GpdQ in complex with (A) profenofos, (B) diazinon and (C) chlorpyrifos.

4. Conclusion

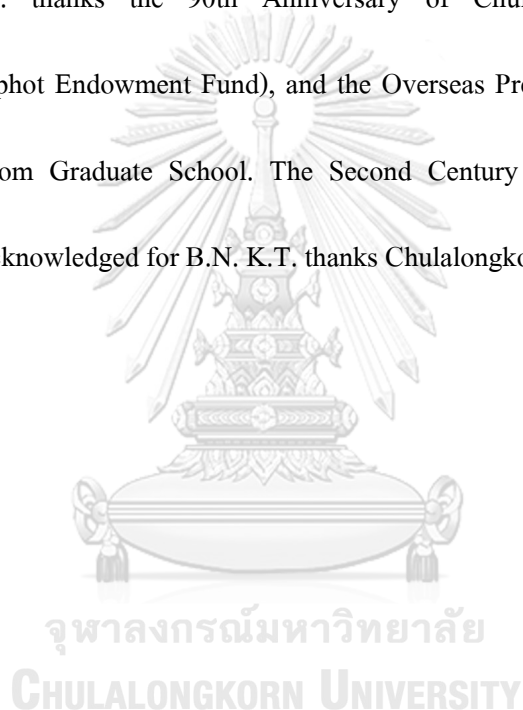
In the present study, the MD simulations of the GpdQ–pesticide complex shed light on the flexibility of the active site of the GpdQ enzyme upon pesticide binding. The coordination chemistry shows how the bulkier pesticide can bind to the enzyme active site since it is comparatively flexible. Our results show that, even though the Fe_{α} and Fe_{β} distance is significantly longer compared to the crystal structure, it is still stable throughout the MD simulation. Also, the distance between the metal ion and N80 along with few other residues around the beta site undergoes conformational changes to accommodate the pesticide bindings. Furthermore, the metal ion at the α site is more stable than the β site. Protein–ligand interactions in terms of binding free energy calculation reveals that electrostatic interactions are predominant for molecular complexation. This study also highlights the residues, which are important for ligand bindings (i.e., P228, Q166, M167, I170, Y230). Computational studies of pesticides, as opposed to the natural substrate mimics provide a greater discrepancy due to bigger size and the formal charges involved in the pesticide. Thus, it would be a better choice to study the binding of the pesticides to the enzyme as it would give a better understanding to prepare mutated enzyme for enhancement of its activity. Lastly, it will be interesting to further investigate how this change in binding conformation will affect the catalytic activity of the GpdQ enzyme toward these pesticides.

Declaration of competing interest

The authors declare that they have no known competing financial interests or personal relationships that could have appeared to influence the work reported in this paper.

Funding

This work was financially supported by the Thailand Research Fund (grant number RSA6280085). N.B. thanks the 90th Anniversary of Chulalongkorn University Fund (Ratchadaphiseksomphot Endowment Fund), and the Overseas Presentations of Graduate Level Academic Thesis from Graduate School. The Second Century Fund (C2F), Chulalongkorn University (CU) is acknowledged for B.N. K.T. thanks Chulalongkorn University for supporting a research visit.



Chapter 2

Manuscript 2

Molecular binding of a different classes of organophosphates to methyl parathion hydrolase from *Ochrobactrum* species

Nayana Bhat¹, Bodee Nutho², Sarinya Hadsadee¹, Alisa Vangnai^{1,3}, Thanyada Rungrotmongkol^{1,4*}

¹*Biocatalyst and Environmental Biotechnology Research Unit, Department of Biochemistry, Faculty of Science, Chulalongkorn University, Bangkok 10330, Thailand*

²*Department of Pharmacology, Faculty of Science, Mahidol University, Bangkok 10400, Thailand*

³*Center of Excellence in Hazardous Substance Management, Chulalongkorn University, Bangkok 10330, Thailand*

⁴*Program in Bioinformatics and Computational Biology, Graduate School, Chulalongkorn University, Bangkok 10330, Thailand*

*Corresponding author. Email: thanyada.r@chula.ac.th, t.rungrotmongkol@gmail.com

Phone: +66-2218-5426. Fax: +66-2218-5418.

(Manuscript in preparation)

จุฬาลงกรณ์มหาวิทยาลัย
CHULALONGKORN UNIVERSITY

Molecular binding of a different classes of organophosphates to methyl parathion hydrolase from *Ochrobactrum* species

Nayana Bhat¹, Bodee Nutho², Sarinya Hadsadee¹, Alisa Vangnai^{1,3}, Thanyada Rungrotmongkol^{1,4*}

¹*Biocatalyst and Environmental Biotechnology Research Unit, Department of Biochemistry, Faculty of Science, Chulalongkorn University, Bangkok 10330, Thailand*

²*Department of Pharmacology, Faculty of Science, Mahidol University, Bangkok 10400, Thailand*

³*Center of Excellence in Hazardous Substance Management, Chulalongkorn University, Bangkok 10330, Thailand*

⁴*Program in Bioinformatics and Computational Biology, Graduate School, Chulalongkorn University, Bangkok 10330, Thailand*

*Corresponding author. Email: thanyada.r@chula.ac.th, t.rungrotmongkol@gmail.com

Phone: +66-2218-5426. Fax: +66-2218-5418.

Abstract:

Methyl parathion hydrolase (MPH) is an enzyme from the metallo- β -lactamase superfamily, which hydrolyses a wide range of organophosphates. MPH has attracted recent attention as a promising enzymatic bioremediator. The crystal structure of MPH enzyme shows a dimeric form, and each subunit contains a binuclear metal ion center. MPH demonstrates metal-ion-dependent selectivity patterns. The origins of this remain unclear but are linked to open questions about the more general role of metal ions in functional evolution and divergence within enzyme super families. We aimed to investigate and compare the binding of different organophosphate pesticides. For this study MPH from *Ochrobactrum* sp. was obtained and molecular docking was performed with different classes of organophosphate pesticides such as

phosphomonoester (methyl paraxon, dichlorvos) and S-substituted thiophosphotriester (profenofos) using Cdocker. Refined pose obtained from molecular docking was chosen for classical MD simulations using AMBER16 for 500 ns. Further, the systems with Cobalt and Zinc metal were compared. D255 and a hydroxyl ion acted as bridging ligand and coordinated with both the metal ions. The alpha metal ion coordinated with D151, H152, D255 and H302. It was found that more buried ion and did not coordinate with the pesticide. Instead, the less buried beta metal ion was found to be coordinated with some pesticides. It was also seen that the coordination of beta metal ion was perturbed to accommodate the bulky pesticides. Computational studies of pesticides as opposed to the natural substrate mimics provide a better understanding due to bigger size and the formal charges involved in the pesticide. The ability of the in-silico analysis presented here could be informative for increasing enzyme stability and activity.

1. Introduction

Organophosphates (OP) have been used for major application in chemical warfare agents and pesticides.¹⁻² OP pesticides accounts for total of 38% of global pesticide consumption.³ OP compounds are the main components of herbicides, pesticides, and insecticides.⁸¹ OP compounds are also the main components of nerve gas. Moreover, OP pesticides residues found in agriculture leads to the environmental pollution. Not just that these chemicals still has significant adverse effects on animals and non-target species including humans because of their acetylcholinesterase inhibitory activity that have a profound effect on the nervous system.⁴⁻⁵ OP pesticides are classified based on chemical structure. For example, phosphotriester comprises of phosphate

center with three O-linked groups such as methyl-paraoxon (MPO) and dichlorvos (DDVP). Whereas, thiophosphotriesters have the sulfur replaced the phosphoryl oxygen such as profenofos (PF).⁸²

The enzymatic bioremediation is known to contribute the hydrolysis of OP pesticides. Substantial enzymes show the identify to promote the degradation of OP pesticides including phosphotriesterase (PTE), organophosphorus hydrolases (OPHs),^{7, 9-13} serum paraoxonase (PONs),¹⁴⁻¹⁶ methyl parathion hydrolases (MPHs),¹⁷⁻²¹ diisopropylfluorophosphate fluorohydrolase (DFPase),²¹⁻²² organophosphate acid anhydrolases (OPAAs),²³⁻²⁴ and Phosphotriesterase-Like-Lactonases (PLLs).³⁰⁻³⁶ The OP-degrading enzyme was first discovered in 1946, which hydrolyzed diisopropylfluorophosphate (DFP).⁵⁸ Later in 1973, it was seen that the soil bacterium *Flavobacterium* sp. (strain ATCC 27551) hydrolyzed the OP diazinon.⁷ *Agrobacterium radiobacter*, *Enterobacter aerogenes*, and *Pseudomonas diminuta* were later observed to have enzymes that degrade OPs.^{39, 44, 46, 57}

Specifically, the methyl paraoxon hydrolases (MPHs) are encoded by *mpd* (methyl parathion degradation) genes. The *mpd* genes were first identified in *Plesiomonas* sp. strain M6 and subsequently in bacterial species such as *Achromobacter*, *Ochrobactrum*, *Stenotrophomonas* and *Pseudomonas*.^{18, 20, 37-38} However, the *mpd* genes does not share sequence homology with other OP-degrading genes. The MPH enzyme is a dimeric protein as shown in Figure 1, and each subunit contains a mixed hybrid binuclear zinc center.⁸³

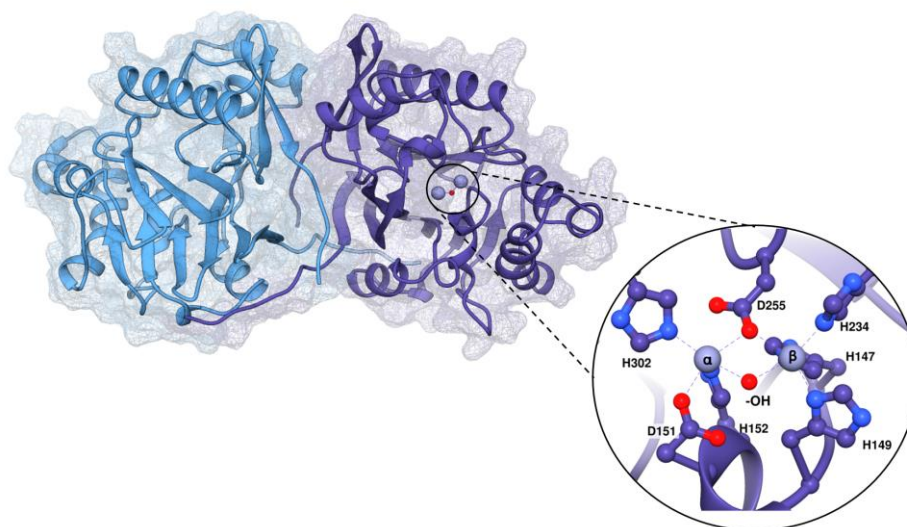


Figure 1. The 3D structure of homodimer MPH, in which chain A and B are shaded by deep blue and light blue colors, respectively. The close-up regions for active site; Zn metal ions with its coordinating amino acids

The monomer structure is composed of $\alpha\beta/\beta\alpha$ sandwich typical of the metallo-hydrolase/oxidoreductase fold. Two internal mixed β -sheets are flanked either side by three solvent-exposed α -helices. Each subunit is composed of a β -lactamase-like domain, which includes the binuclear metal center. The binuclear metal site is located between the two β -sheets and is surrounded by two $\alpha\beta$ -loops. The residues W179, F196 and F119 are three residues that create an aromatic cluster at the entrance of the catalytic center.⁸³ It is seen that Zn^{2+} is the native metal ion for this enzyme. However, the metallo- β -lactamase (MBL) super family enzymes can be constituted with other metal ions such as Fe^{2+} , Mn^{2+} , Co^{2+} and Ni^{2+} .⁸³⁻⁸⁵

Computationally studies are carried out to understand the mechanism of this enzyme.⁸⁶

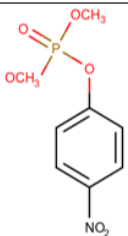
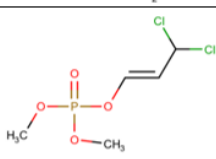
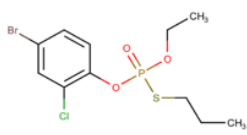
First, nucleophilic attack by terminal hydroxide ion occurs. Next, the bulky substrate by using of

the large active site volume of MPH binds in-line for nucleophilic attack on the organophosphate.

The nucleophilic attacks the aryl ester, which requires very different binding modes for the substrates, resulting also in transition state stabilization from different active site residues.

Here in this study, we present the substrate binding mechanism of MPH enzyme towards different classes of OP pesticides such as phosphotriesters, thiophosphotriesters. The substrate binding mechanism of dichlorvos (phosphotriester) and profenofos (thiophosphotriesters) is compared with natural substrate methyl paraxon (phosphotriester). The molecular structure is as depicted in in Table 1. The promiscuity of the metal ion with respect to cobalt and zinc is also analyzed with respect to binding of these substrates. Since recently this enzyme is known to be evolved for its the ability to hydrolyze a wide range of man-made organophosphates. The binding mode of the substrate for this is key to enzyme catalysis. There have been very less computational studies carried out on this enzyme that elucidates the mechanism of substrate binding. The information presented in here could provide detailed insights of OPs binding to the enzyme and how the active site modifies itself to fit in various classes of OP pesticides.

Table 1. Chemical structures of different class of organophosphate compounds

Name	Name	Structure	Bond	R-
Phosphotriester	Methyl-Paraxon		P-O	Dimethyl
	Dichlorvos			
Thiophosphotriester (S-substituted)	Profenofos		P-O P-S	Ethyl, propyl Dimethyl

2. Computational Methods

2.1 System preparation and Molecular Docking

The three-dimensional structures of MPH from *Ochrobactrum* sp. have not been resolved yet. The sequence alignment between the MPH from *Ochrobactrum* sp. and *Pseudomonas* sp. was performed by BLAST.⁸⁷⁻⁸⁸ Since the similarity was 99.7% (One residue mismatch in signal peptide sequence) the Zn(II) bound MPH from *Pseudomonas* sp. WBC-3 with a 2.4 Å resolution (accession code 1P9E) was used as initial native structure.⁸³ Initial native structure, Zn metals were contained in structure of MPH. To create cobalt containing MPH, Zn(II) were replaced with cobalt(II) in discovery studio. The protonation states of all ionizable amino acids (D, E, K, R and H) were assigned at pH 8.0 using PROPKA3.1.⁶¹ Their environments were also visually explored by considering the possibility of hydrogen bonding with the surrounding residues. The charges

were calculated using Gaussian. The AMBER ff14SB force field was applied for the protein.⁶² Methyl paraoxon, dichlorvos and profenofos were built using the Gaussview6.0 program. Substrate parameterization for these pesticides were generated by antechamber module implemented in AMBER16 with general AMBER force field (GAFF) by parmchk program.⁶⁴ Partial charges were set to fit the electrostatic potential generated at the HF/6-31G(d) level by the RESP model. For the MD simulations all OP pesticides were docked with 100 independent runs into the active site of the MPH using CDOCKER module⁶⁵ in the Accelrys Discovery Studio 2.5 Accelrys Inc for MD simulations. The amino acid residues surrounding the metal ions such as H147, H149, H234, D255 and H302 were chosen to define the binding site for the docking process. The lowest distance between the phosphodiester bond and the metal ion were selected to start for MD simulations. Additionally, we also checked the orientation of the pesticide to be in-line for nucleophilic attack. The suitable docked conformers for MPH with each pesticide molecule were selected for subsequent molecular dynamics (MD) simulation. Afterward, the missing hydrogen atoms were added by using the LeaP module of AMBER16. Each system was immersed in a pre-equilibrated truncated cubic box of TIP3P water molecules with an internal offset distance of 10 Å. The box dimension was of $115 \times 115 \times 115 \text{ \AA}^3$, with approximately 20300 water molecules. All systems were neutralized with explicit Cl⁻ counterions. Calculations were performed with ff14SB built in Amber force field and TIP3P water model.⁶⁶ Geometry optimization was carried out in two steps. Firstly, the solvent and counter ions were initially minimized by 1500 steps of steepest descent (SD) and 3000 steps of conjugate gradient (CG)

methods, while the other molecules were restrained using a force constant of $500 \text{ kcal/mol}\cdot\text{\AA}^2$. The second step unrestrained minimization of all the atoms in the simulation cell was carried out. The protein was minimized by SD (1000 steps) and CG (2500 steps) methods with a constrained solvent. Finally, the SD (1000 steps) and CG (2500 steps) minimizations were fully applied to the whole system. Moreover, the systems were heated under constant volume and periodic boundary conditions from 0 to 303 K.

2.2 Molecular dynamics (MD) simulations

MD simulations were simulated based on the standard procedure⁶⁷ using isothermal–isobaric ensemble (NPT) at a constant pressure of 1 atm equilibrated at 303 K for 500 ns. The calculated simulation time step was set to 2 fs under periodic boundary condition. Hydrogen bonds restrain in structure for their equilibrium lengths were set by the SHAKE⁶⁸ algorithm. The particle-mesh of Ewald's summation method⁶⁷ was used for non-bonded interactions, a cut of at 10 Å was performed. The constant temperature and pressure were controlled using a Langevin dynamics⁶⁹ and Berendsen barostat⁷⁰, respectively. MD simulations of the complexes was performed by the AMBER16 software package coupled with the PMEMD module.⁷¹ The trajectories were collected for every 10 ps. For the RMSD calculations the CPPTRAJ package was provided in Amber tools was used to generate trajectories for each residue and at an amino acid resolution. The individual chain of MPH (chain A and chain B) and the pesticide was plotted along simulation time, as shown in Supplementary Figure 1. The RMSD results of all the MPH–pesticide complexes were found to be fairly stable. For all future analysis, last 50 ns (450–

500 ns) of MD simulations were considered. Trajectory analysis was carried out using cpptraj, which is part of the AMBER16 package.⁷² Binding free energy and per residue energy contribution were calculated by MM/PBSA method.⁷³

3. Results and discussion

3.1 Substrate binding

Methyl parathion hydrolase enzyme is a soil dwelling bacterium that uses methyl parathion as sole source of carbon and nitrogen. In this study, the substrate binding of *Ochrobactrum* MPH with three different OPs pesticides including methyl paraxon, dichlorvos and profenofos were determined and compared. Additionally, the MPH were simulated using cobalt and zinc. In this work, two series of MD simulations was carried out. For the first one, to cobalt metal ion was bound in the active site of MPH and for the second one with zinc metal ion. We docked three pesticides in the active site of zinc bound and cobalt bound MPH in cDocker embedded in discovery studio. 100 poses were obtained for each system and the pose with lowest distance between the pesticide and the metal ion. Along with that, the lowest interaction energy was considered as initial structure. The active site is composed of His and Asp residues surrounding the metal ions.⁸³ The hydrophobic pocket is also present that helps to accommodate the substrate. The substrate was fitted in the pocket. **Figure 2** depicts the selected docked structures. It must be noted that there is a water molecule close to the two metal ions. Therefore, from the crystal structure that was retained for its role in the catalysis. All the six systems had

good interaction energy (**Table 2**) ranging between -32 to -36 kcal/mol. Thus, six systems were used as initial structures for molecular dynamics simulations.

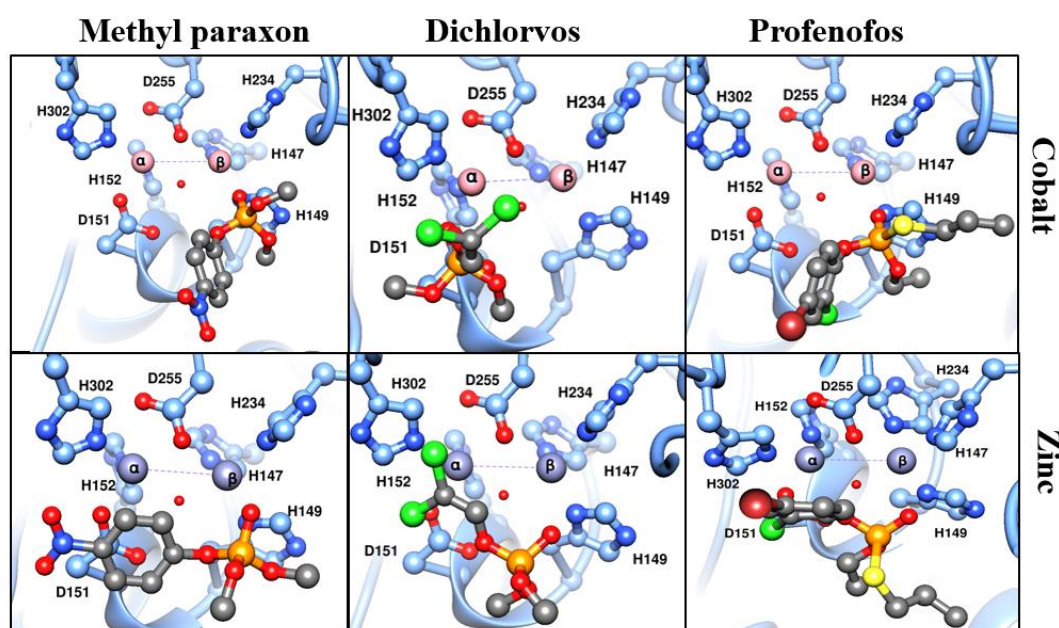


Figure 2. Active site of initial structures for MD simulations of all the systems

Molecular dynamics simulations were carried out in triplicates for all the 6 systems for 500 ns using AMBER16. The system stability was analyzed by RMSD calculations, and it was found that all the systems were stable throughout the simulations (supplementary figure 1). The MPH enzyme contains 2 metal ions in its active site. As shown in **Figure 2**, the active sites of two enzymes are very similar, but both enzymes have different divalent cation metals, namely Co(II) and Zn(II). The bond distance of two metals ion were investigated. The distance and position of two metal ions from one and another can be calculated to deduce the stability of both the metal ions and hence the probability of higher enzyme activity. In the structure with Co(II) metal ion the distance between the two metal ions in the crystal structure was found to 3.5 Å. Throughout

the stimulations the distance between the Zn metal ions was found be stable between 3.0 - 3.25 Å. Whereas the cobalt metal ions had a distance in the range of 3.25 - 3.6 Å. The difference in the distance was attributed to the radius of the metal ion. The distance between the metal ions and the nature of metal ions was found to very important specifically when nonspecific substrates were catalyzed. Obviously, cobalt-MPH systems wherein the distance between the metal ions were slightly higher in dichlorvos comparison to the methyl paraxon and profenofos. Besides, the best results of the three replicates are considered.

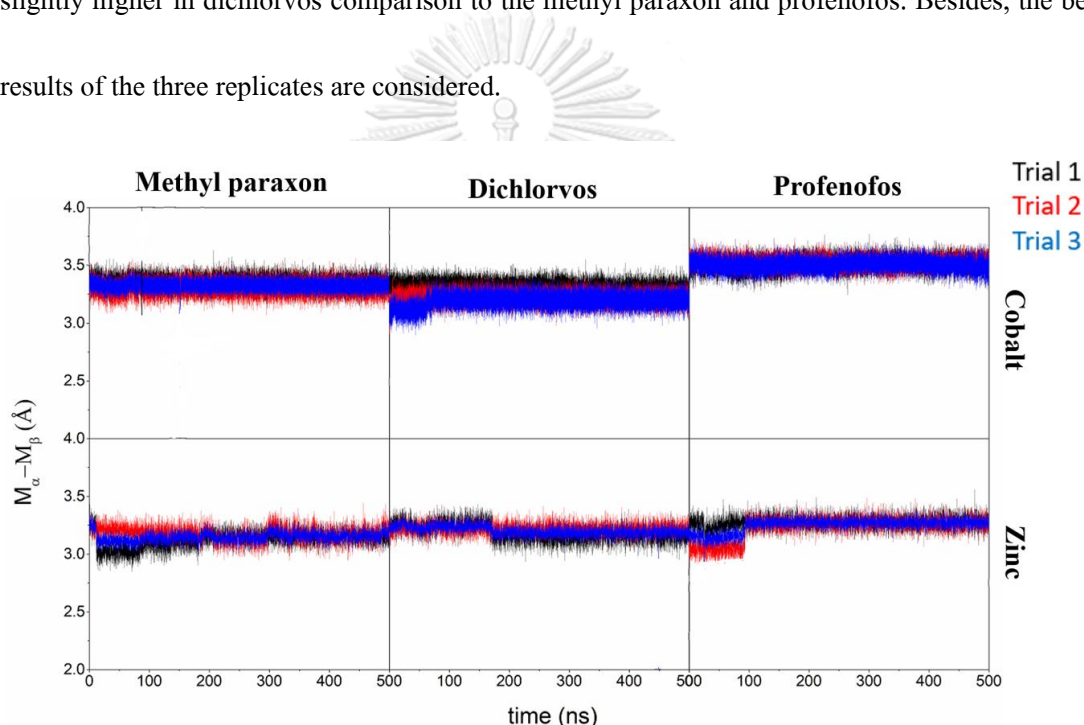


Figure 3. Distance between α and β ions located in the MPH active site in complex with organophosphate pesticides

The active structure of the enzyme consists of a bi-nuclear metal ion coordinated to aspartate and histidine residues. The alpha metal ion is embedded deep inside with D151, D255, H152 and H302. In contrast, beta metal ion is coordinated to D255, H147, H149 and H234. Both the metal ions are also bridged together by a water molecule which plays a role in hydrolysis of

the substrate. We calculated the bond distance between the metal ions, and its residues (**Table 2**). It was observed that none of the pesticides coordinated with alpha metal ion throughout the simulations. The coordination number of the alpha metal ion varied for the different pesticides. We can hypothesize that this change in the coordination number is due to subtle changes in the geometry which occurs to accommodate the side chains of the substrate. Further, the coordination of the beta metal ion to the amino acids changed completely to accommodate the pesticides. The metal ion lost the coordination with the histidine residues. The coordination distance between the beta metal ions and the pesticides were in the range of 1.90 – 1.98 Å. These results show that the geometric constraints at the beta metal ion could be attributed to the in-line nucleophilic attack on the organophosphate pesticide. These results correspond to the hypothesized mechanism of the enzyme earlier.⁸⁶ However the changes in the coordination number in different pesticide systems can probe that they have different binding strategy.

Table 2. Distance (Å) of the α and β ions with surrounding amino acids, pesticide, and water.

ALPHA metal ion	Metal ion	D151	H152	D255	H302	ROH (Crystal water)	Pesticide
Methyl paraxon	Cobalt	1.83 ± 0.04	2.72 ± 0.38	1.87 ± 0.06	2.21 ± 0.06	1.80 ± 0.12	3.84 ± 0.26
	Zinc	1.79 ± 0.04	3.53 ± 0.33	1.79 ± 0.04	4.04 ± 0.83	1.79 ± 0.09	5.11 ± 0.06
Dichlorvos	Cobalt	1.87 ± 0.05	2.30 ± 0.21	4.17 ± 0.20	2.10 ± 0.12	1.77 ± 0.04	3.98 ± 0.33
	Zinc	1.75 ± 0.03	2.01 ± 0.11	1.74 ± 0.03	2.04 ± 0.11	1.79 ± 0.05	4.50 ± 0.04
Profenofos	Cobalt	1.85 ± 0.05	2.07 ± 0.08	1.86 ± 0.08	3.21 ± 0.05	1.78 ± 0.44	3.31 ± 0.04
	Zinc	1.84 ± 0.05	4.88 ± 0.58	1.83 ± 0.05	2.18 ± 0.18	1.75 ± 0.04	4.47 ± 0.69

BETA metal ion	Metal ion	H147	H149	H234	D255	ROH (Crystal water)	Pesticide
Methyl paraxon	Cobalt	5.36 ± 0.27	4.55 ± 0.42	6.06 ± 0.21	1.89 ± 0.06	1.80 ± 0.04	1.95 ± 0.04
	Zinc	5.05 ± 0.55	4.22 ± 0.52	6.84 ± 0.68	1.81 ± 0.04	1.80 ± 0.04	1.90 ± 0.06
Dichlorvos	Cobalt	4.69 ± 1.28	5.53 ± 0.66	5.29 ± 0.76	2.74 ± 0.76	1.78 ± 0.04	1.91 ± 0.10
	Zinc	6.50 ± 0.37	2.33 ± 0.16	8.12 ± 0.83	1.80 ± 0.05	1.78 ± 0.04	1.90 ± 0.04
Profenofos	Cobalt	4.90 ± 0.33	3.65 ± 0.83	6.36 ± 0.30	1.86 ± 0.05	1.81 ± 0.04	1.98 ± 0.08
	Zinc	1.99 ± 0.07	2.02 ± 0.08	1.99 ± 0.07	1.76 ± 0.04	1.73 ± 0.03	1.96 ± 0.55

3.2 Binding affinity and key binding residues

The binding affinities of the three pesticides in presence of zinc and metal ion in the active site was calculated by MM/PBSA method. The stable MD trajectories (450-500 ns) was used for energy calculations. A total of 500 snapshots were taken from the last 50 trajectories to analyze the binding energy. The counterions and water molecules were stripped. The final binding free energy was determined as the average of all the snapshots and the standard errors are also reported (**Table 3**). The metal ion dependent binding changes was observed from the results. The results showed that the binding free energy of the cobalt-MPH was 3-5 times more when compared to zinc -MPH systems. However, in the case of profenofos the zinc-MPH showed better binding than the cobalt MPH. These results indicated that the different classes of organophosphates could have different mode of substrate binding.

Table 3. Binding free energy of all the systems calculated by MM/PBSA method

	ΔG_{bind} (kcal/mol)	
	Cobalt	Zinc
Methyl paraxon	-11.32 \pm 6.28	-02.81 \pm 0.91
Dichlorvos	-14.03 \pm 2.06	-04.08 \pm 1.04
Profenofos	-20.27 \pm 2.34	-25.67 \pm 1.31

To understand the role of each amino acid, the contribution to the substrate binding, per-residue binding free energy was calculated. **Figure 5** depicted the contribution of individual amino acid residues in the chain A towards substrate binding. The residues V65, L67, F85, F196 and L273 played important role in substrate binding. It must be noted that F85 and F196 were residues present in substrate binding pocket. These residues form π - π or π -alkyl interactions with the substrate. From these results it could be deduced that all three pesticides can bound to MPH enzyme with cobalt or zinc metal ion and could subsequently undergo hydrolysis via nucleophilic attack.

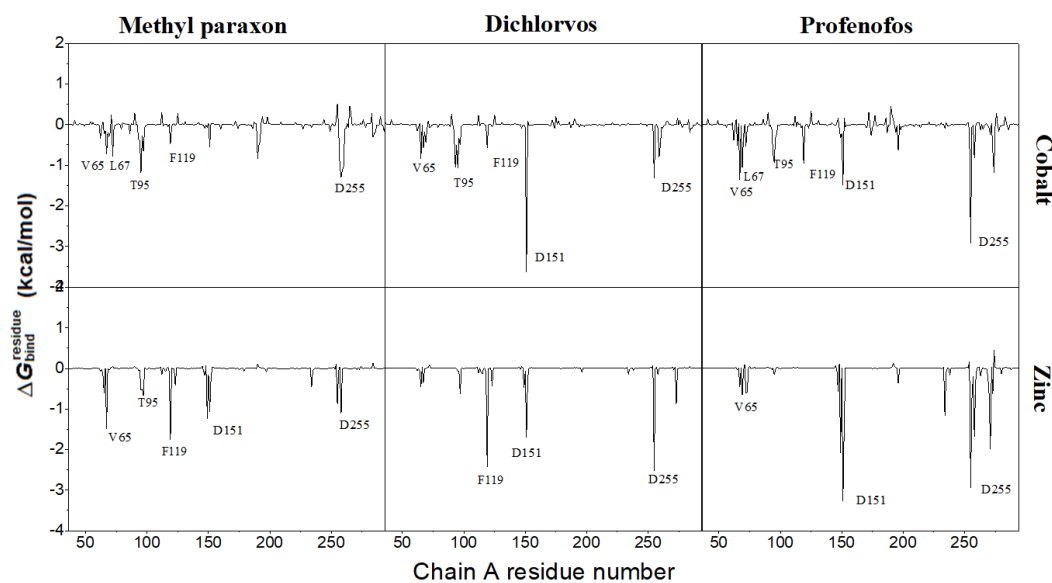


Figure 5. Per-residue decomposition free energy ($\Delta G_{\text{bind}}^{\text{residue}}$) of all the systems of the MPH

Conclusion

The metallohydrolase enzymes used for bioremediation must have two intrinsic properties. i.e., good stability of the metal ions and wide range of substrate specificity. In this research we aimed to study the stability of metal ion and understand the substrate binding mechanism of nonspecific substrates in presence of two different metal ions. Both zinc and cobalt metal ion showed good stability throughout the simulations and aided in substrate binding. All the organophosphate pesticides could bind well in the active site and in the confirmation that allows successful the substrate catalysis. The difference in metal ion activity could be attributed by electrostatic properties of the metals themselves. From the analysis of our simulations, it is evident that subtle changes occur in the coordination geometry to accommodate the substrates for

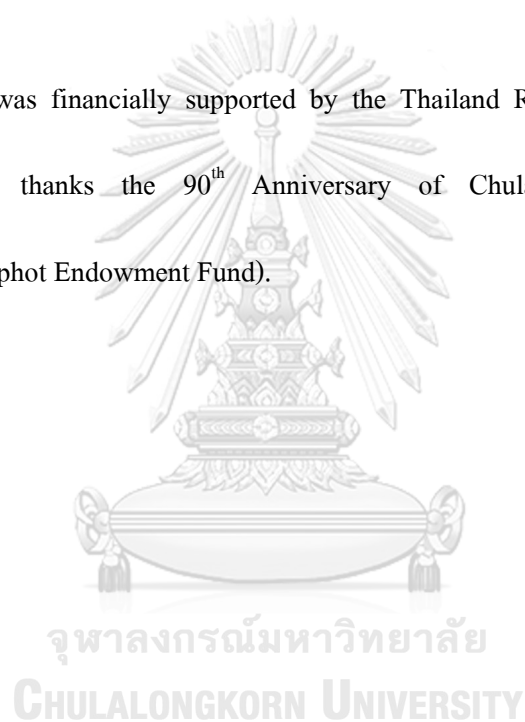
subsequent catalysis. These results could pave way for successfully using the MPH enzyme as an excellent bioremediator.

Conflict of interest

The authors have declared that these are no conflict of interest.

Acknowledgement

This work was financially supported by the Thailand Research Fund (grant number SA6280085). N.B. thanks the 90th Anniversary of Chulalongkorn University Fund (Ratchadaphiseksomphot Endowment Fund).



Chapter 3

Manuscript 3

Kinetics and in silico studies of carbamates as inhibitors of methyl parathion hydrolase

Nayana Bhat¹, Alisa Vangnai^{1,2*}, Thanyada Rungrotmongkol^{1,3*}

¹*Biocatalyst and Environmental Biotechnology Research Unit, Department of Biochemistry, Faculty of Science, Chulalongkorn University, Bangkok 10330, Thailand*

²*Center of Excellence in Hazardous Substance Management, Chulalongkorn University, Bangkok 10330, Thailand*

³*Program in Bioinformatics and Computational Biology, Graduate School, Chulalongkorn University, Bangkok 10330, Thailand*

*Corresponding author. Email: alisa.v@chula.ac.th, thanyada.r@chula.ac.th

Phone: +66-2218-5426. Fax: +66-2218-5418.

(Manuscript in preparation)

จุฬาลงกรณ์มหาวิทยาลัย
CHULALONGKORN UNIVERSITY

Kinetics and in silico studies of carbamates as inhibitors of methyl parathion hydrolase

Nayana Bhat¹, Alisa Vangnai^{1,2*}, Thanyada Rungrotmongkol^{1,3*}

¹*Biocatalyst and Environmental Biotechnology Research Unit, Department of Biochemistry, Faculty of Science, Chulalongkorn University, Bangkok 10330, Thailand*

²*Center of Excellence in Hazardous Substance Management, Chulalongkorn University, Bangkok 10330, Thailand*

³*Program in Bioinformatics and Computational Biology, Graduate School, Chulalongkorn University, Bangkok 10330, Thailand*

*Corresponding author. Email: alisa.v@chula.ac.th thanyada.r@chula.ac.th

Phone: +66-2218-5426. Fax: +66-2218-5418.

Abstract:

Methyl Parathion Hydrolase from *Ochrobactrum* sp is widely used as bioremediator to breakdown a broad range of harmful organophosphate pesticides. However, the synergism or inhibition of this enzyme is not well understood. In this study, we aimed to investigate the effect of carbamate pesticides such as carbaryl and carbofuran towards the MPH enzyme. Enzyme kinetics analysis showed uncompetitive or mixed type of inhibition at higher concentrations of carbamates. To obtain molecular insights the mechanism of action of these carbamates, each compound was docked into the three possible binding pockets of MPH identified by POCASA 1.1. The 200-ns molecular dynamics simulations revealed that the pocket 2 was found to be the

most preferable binding site for both carbamates. S87, A260, L303, R319, F320, and P322 served as the key residues for inhibitor binding.

Keyword: methyl parathion hydrolase; carbamates; computational simulations; enzyme kinetics

1. Introduction

Pesticide poisoning in recent years is the most common and important problem. Around 2.5 million tons of pesticides including organophosphates and carbamates are used globally.⁸⁹⁻⁴⁴ Methyl parathion hydrolase (MPH; E.C.3.1.8.1), a dimeric enzyme with binuclear metal ion found in soil-dwelling bacteria, breaks down methyl parathion to dimethylthiophosphoric acid and p-nitrophenol (yellow coloured product).^{17, 83, 90-91} MPH enzymes are translated from *mpd* (methyl parathion degrading) genes.⁹² They are known to degrade a variety of organophosphate pesticides, hence can be considered as an excellent enzyme for bioremediation.

The crystal structure of MPH from *Pseudomonas* sp. WBC-3 is well elucidated with PDB ID 1P9E. MPH belongs to metallo- β -lactamase super family.⁸³ It consists of two subunits, and each subunit includes a binuclear metal center (Figure 1). The two metal ions, Cd^{2+} and Zn^{2+} , are 3.5 Å apart and are surrounded by seven residues and two water molecules. The buried metal ion (α) is coordinated with D151, H152, H302 and bridging ligand D255 along with a water molecule. The more solvent exposed ion (β) is coordinated to three histidine residues namely H147, H234, and H149, as well as the bridging D255 and water. Apart from these important residues, there are three hydrophobic residues F119, W179 and F196 in the pocket, which the leaving group of pesticide interacts with.^{83, 90} MPH enzyme can have a wide array of metal ions.

Metal ion selectivity patterns have been studied to elucidate the mechanism for the hydrolysis. The five different transition metal ions Fe^{2+} , Zn^{2+} , Mn^{2+} , Co^{2+} and Ni^{2+} are found to bind with MPH, and no major structural changes occurring during metal substitution⁸⁶. This would mean the selectivity of the enzyme towards metal ion is inherent to the electrostatic properties of the metal ion and the metal ion geometry.

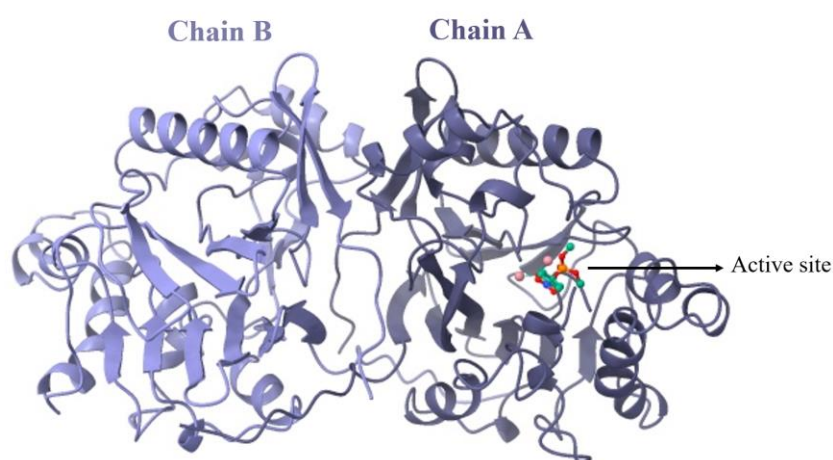


Figure 1. 3D structure of the MPH in complex with methyl paraxon substrate in the active site from molecular docking study, where the chains A and B are shaded by grey and blue, respectively.

Although, the details of MPH structure and its functions have been reported, the information regarding uncompetitive inhibition is lacking. Carbofuran and carbaryl (Figure 2), the carbamates widely used in agriculture worldwide with similar mechanism of action as organophosphorus pesticides⁹³⁻⁹⁴, were focused in the present work. *In vitro* enzyme kinetics in a combination with *in silico* studies were applied to reveal the inhibition mechanism and binding

pattern of these two carbamates. Inhibitor binding studies were sought to anticipate that inhibitors occupied to a distinct cavity and thus providing the topological information of the key residues at binding site along with their contributions for incoming inhibitor.

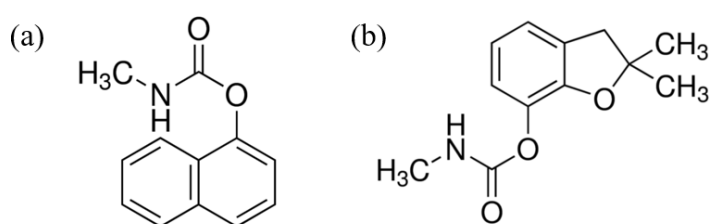


Figure 2. Chemical structures of carbamate pesticides: (a) carbaryl and (b) carbofuran

2. Materials and methods

2.1. Chemicals and reagents

Organophosphate pesticide (methyl paraoxon) and carbamates (carbaryl and carbofuran) in standard form were purchased from Sigma (St. Louis, MO, USA) with declared purity from 95 to 99.2%. Methyl paraoxon and carbamate stock solution were prepared in absolute ethanol and stored in the dark at 4 °C.

2.2. Enzyme activity assay

MPH enzyme hydrolyses methyl-paraoxon to release p-nitrophenol (yellow colored product) which can be measured at 410 nm ($\epsilon_{410} = 11,933 \text{ M}^{-1} \text{ cm}^{-1}$ for p-nitrophenol). A UV-Visible spectrophotometer was used to measure the change in color. 40 mM methyl-paraoxon was

added in the cuvette to obtain the final concentration between 0.2-0.8 mM. To this 50 mM Tris-HCl (pH 8) buffer containing 0.1 mM CoCl₂ was added to bring the total volume to 740 μL. The reaction was initiated by addition of 10 μL of 1:20 diluted crude enzyme. The cuvette was placed in the spectrophotometer, the reaction was proceeded for 10 mins and the absorbance was measured every 30s. Assays were performed at room temperature.

Enzyme activity was defined as Unit (micromole of methyl-paraoxon hydrolyzed to p-nitrophenol per minute) per milliliter.⁹⁵ Specific enzymatic activity was expressed as unit/milligram of protein as follow.

Enzyme activity (Unit.mL⁻¹) = (A₄₁₀ x Volume of assay x Dilution factor) / (Extinction coefficient of p-nitrophenol x Volume of enzyme x Time)

2.3. Kinetics of inhibition of MPH by carbamates

The enzyme inhibition assay was performed spectrophotometrically. The kinetic constants were determined by performing enzymatic assays by varying substrate concentrations of 0.2-0.8 mM for fixed enzyme concentration. The inhibitor concentration ranged between 0.01 – 0.05 mM. Lineweaver-Burk plots were generated for carbaryl and carbofuran.

2.4. Prediction of ligand binding site

To predict ligand binding site of MPH, the pocket identification of the enzyme was performed on the crystal structure of MPH (1P9E.pdb) using POCASA 1.1 software.⁹⁶ The water molecules were removed, and the Zn²⁺ at both α and β position was replaced with Co²⁺. The

probe radius was set to 4 Å. The probable ligand binding sites were measured for their pocket size.

2.5. Molecular docking of carbamates

MPH structure was submitted to H++ server⁹⁷⁻⁹⁸ to adjust the protonation state of all ionizable residues at pH 8.0. The structures of two carbamates (carbofuran: CID 2566 and carbaryl: CID 6129), and the natural substrate (methyl paraxon: CID 13708) were obtained from PubChem database. The geometry of ligands was optimized by HF/6-31G(d) level of theory using gaussian09 program.⁶³

FlexX docking was chosen to perform blind protein-ligand docking⁹⁹ of carbofuran carbaryl, and methyl paraxon. After the generation of 100 docking poses, all docked structures were clustered. Based on number of docking structure and docking energy, three proper clusters at different binding sites were considered for analysis. The structure with lowest docking energy from each cluster was selected for performing MD simulations.

2.6. Molecular dynamics simulations of carbamates/MPH complexes

All-atom force field ff19SB was used to describe the protein-ligand complex.⁶² ESP charges were calculated and RESP charges were assigned using antechamber module and the general amber force field (GAFF) was applied.⁷² LeAP module was used to add missing atoms and TIP3P water model in octahedral box of 10 Å was used to solvate the system.⁶⁶ The systems were then minimized in 2 steps. First, steepest descent (SD) of 1500 steps and conjugate gradient (CG) of 3000 steps was applied to the protein complex followed by the SD (1000 steps) and CG

(2500 steps) to the whole system. A force constant of 500 kcal/mol-Å^2 was maintained throughout the minimization. To perform MD simulations the system was heated from 0 to 303 K for 500 ps, isothermal–isobaric ensemble (NPT) at a constant pressure of 1 atm. A 2-fs time set up was used under periodic boundary condition. To constrain covalent bonds involving hydrogen bonds SHAKE algorithm⁶⁸ was used and treatment of long-range electrostatic interactions (10 Å cut-off distance) was done by particle-mesh of Ewald’s summation method, the Langevin dynamics⁶⁹ and Berendsen barostat⁷⁰ were used to control temperature and pressure respectively. Finally, 100 ns molecular dynamics simulations in AMBER16 software package with PMEMD module was performed. At every 10 ps the trajectories were collected. The root-mean square deviation (RMSD) was calculated with CPPTRAJ module of AMBER16. The binding free energy with entropy were calculated using molecular mechanics/ Poisson–Boltzmann surface area (MM/PBSA) approach.⁷³

2.5. Statistical analysis

The inhibition experiments were done in triplicates. The results were expressed as the mean \pm standard deviation (SD). One-way analysis of variance (ANOVA) was carried out to evaluate statistical significance (< 0.05 significance).

3. Results

3.1 Enzyme kinetics

In this study, the breakdown of methyl paraxon by MPH was measured spectroscopically by measuring the concentration of the p-nitrophenolate (yellow product) at 410 nm. The initial velocity (V) of the hydrolysis reactions catalyzed by methyl parathion hydrolase was measured at various substrate concentrations (0.2-0.8 mM).

To determine the type of inhibition of carbaryl and carbofuran, its MPH activity was analyzed by varying inhibitor concentration between 0.01 – 0.1 mM. The initial velocity was plotted in Lineweaver-Burk plot from the MPH activity assay at different concentration of methyl paraxon. From the Lineweaver-Burk plots it can be deduced that the inhibition type of carbaryl is mixed type or uncompetitive mode. As seen in (**Figure 3** and **Table 1**), with increasing concentration of the carbaryl concentration the K_m values decreased and concomitantly the V_{max} values also decreased. Similarly, carbofuran also exhibits similar inhibition. However, at low concentration of the inhibitor the activity of the enzyme activity increases slightly. The apparent increase in K_m on the inhibitor binding favors the binding of inhibitor to the enzyme substrate complex. These compounds are thereby determined to be mixed type of inhibition, and they probably bind to site distinct from the substrate. To validate this hypothesis, molecular dynamic studies were performed in comparison with enzyme assay data. The K_i values as determined by Dixon plots (**Supplementary Figure 2.**) for carbaryl and carbofuran were 0.16 and 0.30 mM respectively.

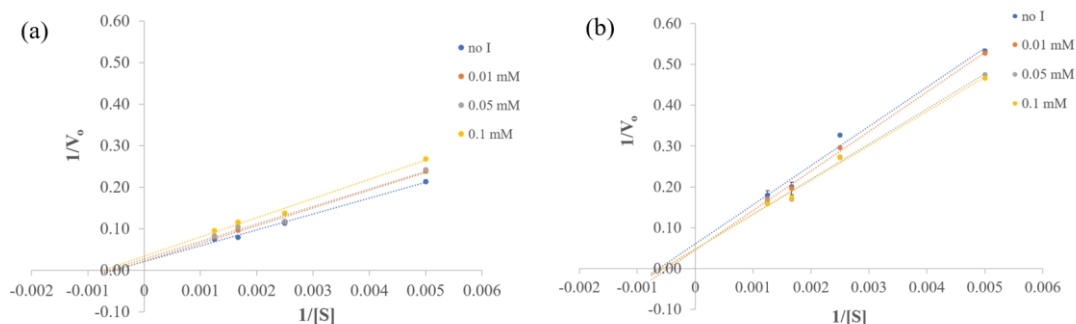


Figure 3. Determining the type of inhibition for (a) carbaryl and (b) carbofuran

Table 1. Michaelis-Menten constants for carbaryl and carbofuran

Inhibitor concentration (mM)	Carbaryl		Carbofuran	
	Vmax (mM.min ⁻¹)	Km (mM)	Vmax (mM.min ⁻¹)	Km (mM)
0	46.30	1763.38	16.61	1594.24
0.01	44.25	1885.88	21.79	2105.97
0.05	35.97	1513.67	21.05	1806.40
0.1	28.82	1329.48	20.75	1743.61

3.2 Ligand binding site prediction

POCASA (POcket-CAvity Search Application) is an automatic program that implements the algorithm named *Roll* which can predict binding sites by detecting pockets and cavities of proteins of known 3D structure. To detect the potential ligand-binding sites of MPH enzyme, the

protein structure from PDB database (1P9E) was uploaded to POCASA. The probe radius was set to 4 Å and grid size to 1 Å. Five potential ligand binding sites were obtained in the output. As seen in the **Figure. 4** of the binding sites corresponded to the active site of Chain A and Chain B of MPH enzyme. The other two pockets were found in the groove between the two chains. Finally, the last pocket was found close to active site of Chain B.

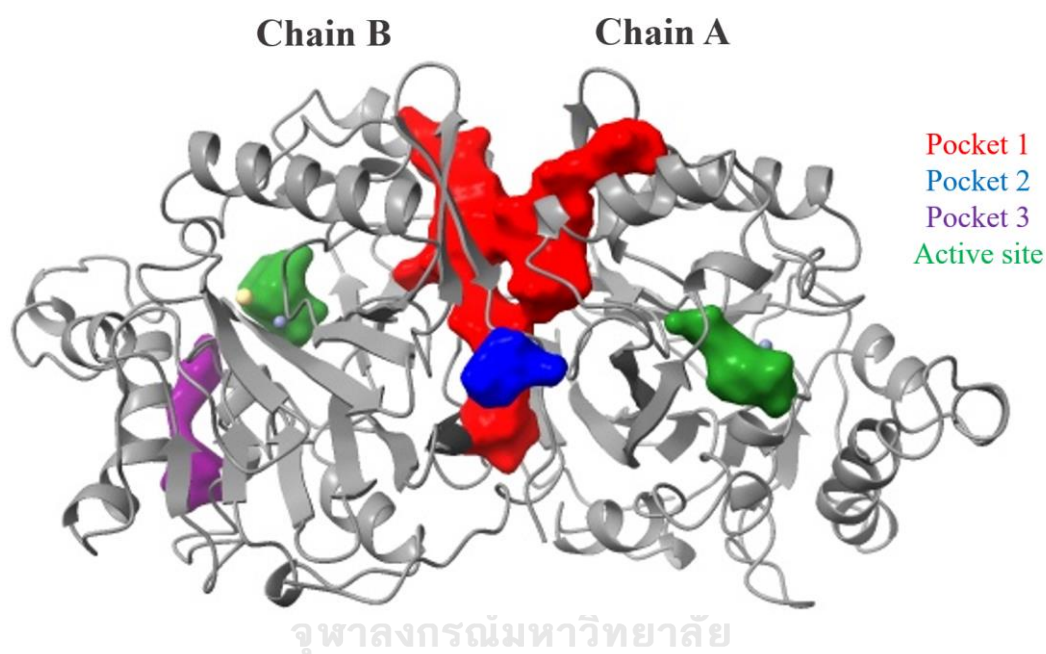


Figure 4. The MPH crystal structure (grey ribbons) and its predicted binding sites (molecular surfaces are rendered): active sites (green), and other binding sites (red, blue, and purple).

3.3 Molecular docking

To determine if the inhibitors docked to the identified pockets, molecular docking was performed on FlexX. The natural substrate (methyl paraxon) and carbamates (carbofuran and carbaryl) were docked blindly, and 100 independent poses were obtained. All the 100 poses from each ligand were clustered based on the binding site as shown in Figure 5. It was seen that of the

100 poses, both carbaryl and carbofuran did not bind to the active site of enzyme. However, in case of methyl paraxon few of the poses were docked at active site. The docking energy and number of docked ligands at each site is shown in **Table 2**. The clustering of poses agreed well with the binding pockets identified by POCASA. It must be noted that in case of carbaryl and carbofuran the ligands clustered predominantly in three different sites. The pose with lowest docking interaction energy were picked for further analysis.

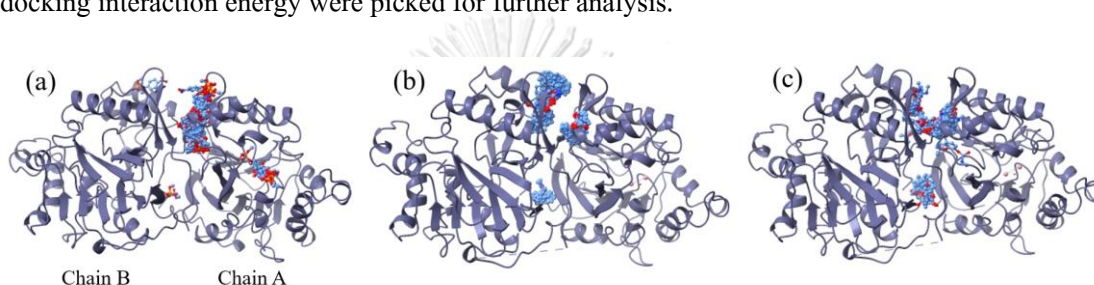


Figure 5. Resulting clusters of computational docking between MPH and (a) methyl paraxon (b) carbaryl and (c) carbofuran

Table 2. Methyl paraxon and carbamate docking clustering results and FlexX docking score

Pocket No.	Methyl Paraoxon		Carbaryl		Carbofuran	
	Number of Docked ligands	lowest docking score (kcal/mol)	Number of Docked ligands	lowest docking score (kcal/mol)	Number of Docked ligands	lowest docking score (kcal/mol)
Active	6	-18.156	-	-	-	-

site						
1 (chain A)	92	-20.286	36	-20.96	82	-23.51
1 (chain B)	1	-14.416	55	-23.27	7	-15.89
2	2	-13.946	4	-24.73	11	-14.11

3.4 Molecular dynamics simulations

In order to further analyze the binding mode and the interaction of the inhibitors with the enzyme, molecular dynamics simulations were carried out for 200 ns in AMBER16. During the simulations we monitored the system stability, the H-bonds, and the binding free energy. The crucial residues that interact with the inhibitor was also monitored. The initial structure and their docking free energy are as shown in **Figure 6**.

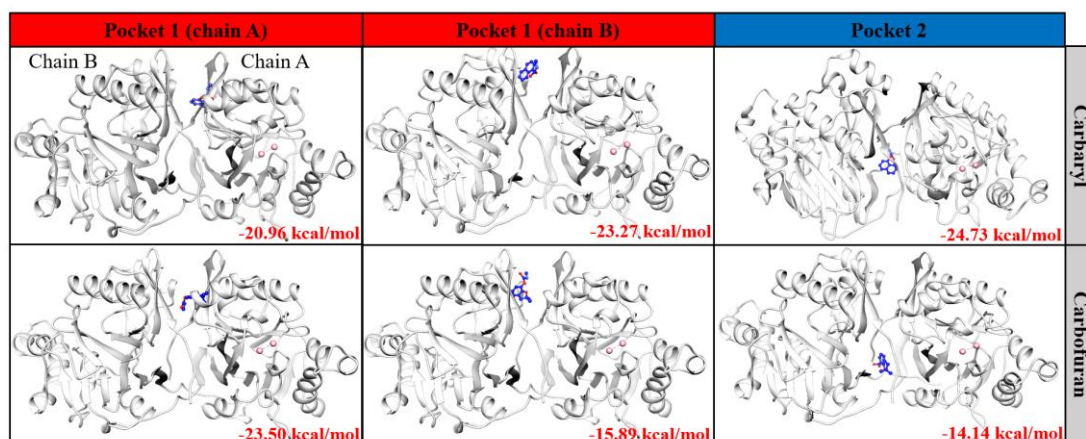


Figure 6. Initial structure of carbaryl and carbofuran bound to three different binding pockets.

The FlexX docking energy is also mentioned.

The RMSD values of backbone residues of Chain A, Chain B and the inhibitor was calculated throughout the simulations. All the 6 systems were found to be stable throughout the simulations and reached equilibrium (**Supplementary figure 1**). However, the RMSD of inhibitor bound to chain B was slightly higher and more stable than the inhibitor in the other two pockets. Further, the initial and final snapshot of MD simulations of all the 6 systems were carried out. It was observed that (**Figure 7**) at the end of simulations the inhibitor embedded deep inside the groove forming stable complexes. In the case of carbaryl the inhibitor moved deeper in the same chain at the end of simulations. However, in case of carbofuran it was seen that the inhibitor

bound to chain A only irrespective of the initial binding site.

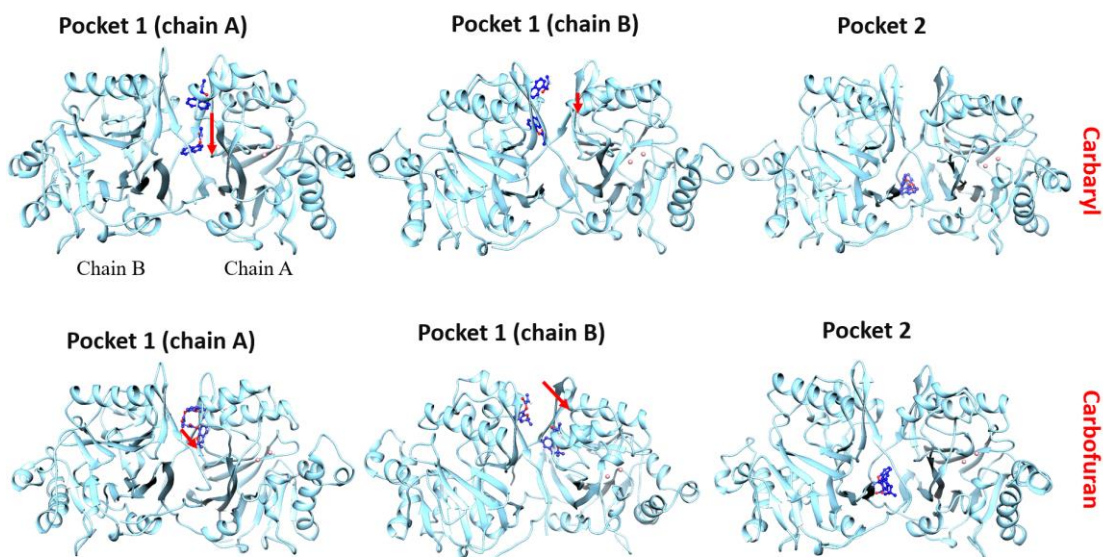


Figure 7. Superimposition of initial and last snapshot in pocket 1 (chain A and B) and pocket 2

Next, the binding free energies of all the systems were calculated by MM-PBSA method. Both carbaryl and carbofuran had good binding in all the three pockets. The binding free energies were mainly contributed by Vander Waal's interaction. It was seen that the binding free energies of the pocket 2 was higher in both the carbofuran (-21.58 ± 3.61 kcal/mol) and carbaryl (-12.54 ± 0.54 kcal/mol). Therefore, for further analysis only inhibitor bound to chain B was considered. The energy components are tabulated in **Table 3**.

Table 3. Binding free energy and its components of carbaryl and carbofuran in pocket 1 of Chain B calculated by MM/PBSA

	Carbaryl	Carbofuran
ΔE_{ele}	-2.91 ± 0.68	-5.05 ± 0.74
ΔE_{vdW}	-22.35 ± 1.97	-29.86 ± 0.81
ΔE_{MM}	-25.27 ± 1.90	-34.91 ± 0.81
$\Delta G_{\text{solv}}^{\text{nonpolar}}$	-4.16 ± 0.19	-4.84 ± 0.03
$\Delta G_{\text{solv}}^{\text{ele}}$	10.99 ± 0.81	13.11 ± 0.81
ΔG_{sol}	6.83 ± 0.78	8.27 ± 0.89
$\Delta G_{\text{solv}}^{\text{nonpolar}} + \Delta E_{\text{vdW}}$	-26.35 ± 0.84	-34.70 ± 0.84
$\Delta G_{\text{solv}}^{\text{ele}} + \Delta E_{\text{ele}}$	8.25 ± 0.42	8.05 ± 0.74
$-T\Delta S$	05.88 ± 0.21	6.55 ± 1.20
ΔG_{bind}	-12.55 ± 0.54	-21.58 ± 1.20

3.4 Interaction analysis

To understand the interactions between the inhibitor and surrounding amino acid residues, per residue energy decomposition and hydrogen bonding were calculated. Per residue decomposition energy gives in-depth understanding of amino acids involved in binding of inhibitor. The inhibitor was found to interact with both Chain A and Chain B of the enzyme. **Figure 7** depicts the

interaction energy of each residue. S87, F264, R319, F320, V321 and P322 residues of chain A and B were found have good interaction with the inhibitors.

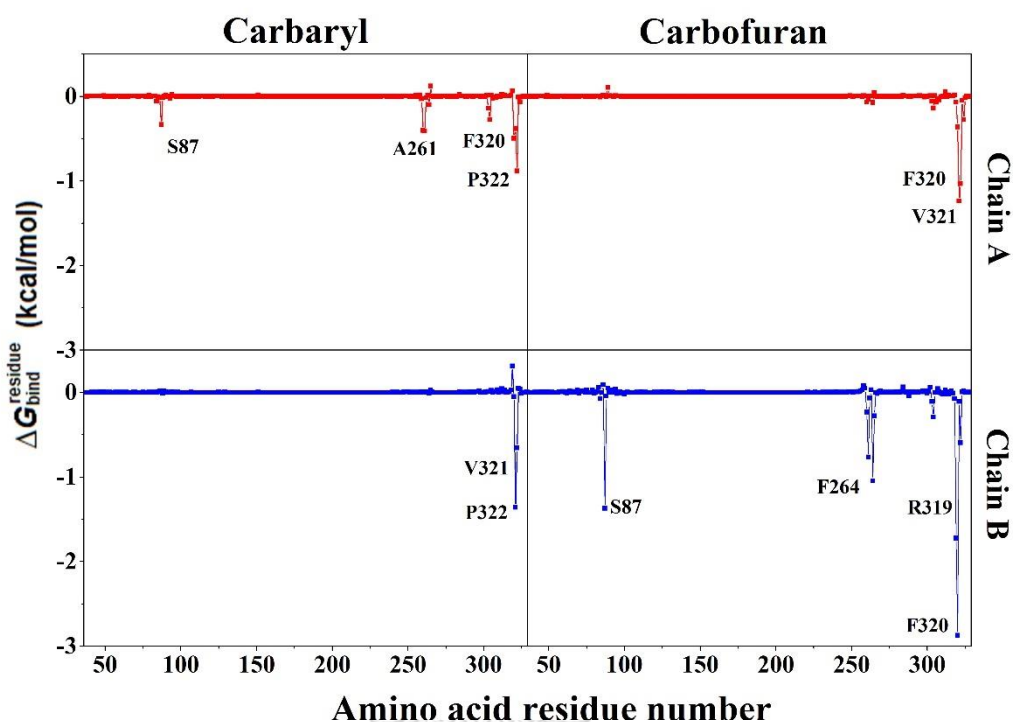


Figure 7. Per-residue decomposition free energy ($\Delta G_{\text{bind}}^{\text{residue}}$) of the systems of the MPH in complex with carbaryl and carbofuran in pocket 1.

Hydrogen bond interactions between the inhibitor and the enzyme was considered further to understand the role of contributing amino acids residues. H-bonds are the key features of the enzyme inhibitor interaction. The carbaryl had a hydrogen bond with S87 and of chain B and R319 and P322 of chain A. However, in the case of carbofuran strong hydrogen bonds were formed with F320 and S87 of chain B of the enzyme. These results can point out to the role as S87 as the hydrogen bond acceptor which could be key to the inhibitory process. Apart from H-bond interactions, the stability of the complex is attributed by π - π and π -alkyl interactions.

The last snapshot of the MD simulations of both carbofuran and carbaryl was used to obtain 2-D interaction image in discovery studio (**Figure 8**). The carbaryl had a π -alkyl interaction with A260 of chain A and carbofuran had π -alkyl interactions with A260, P322, L303 of chain B. Taking all these into account it can be seen that both carbaryl and carbofuran interact well in the binding pocket and could induce inhibition.

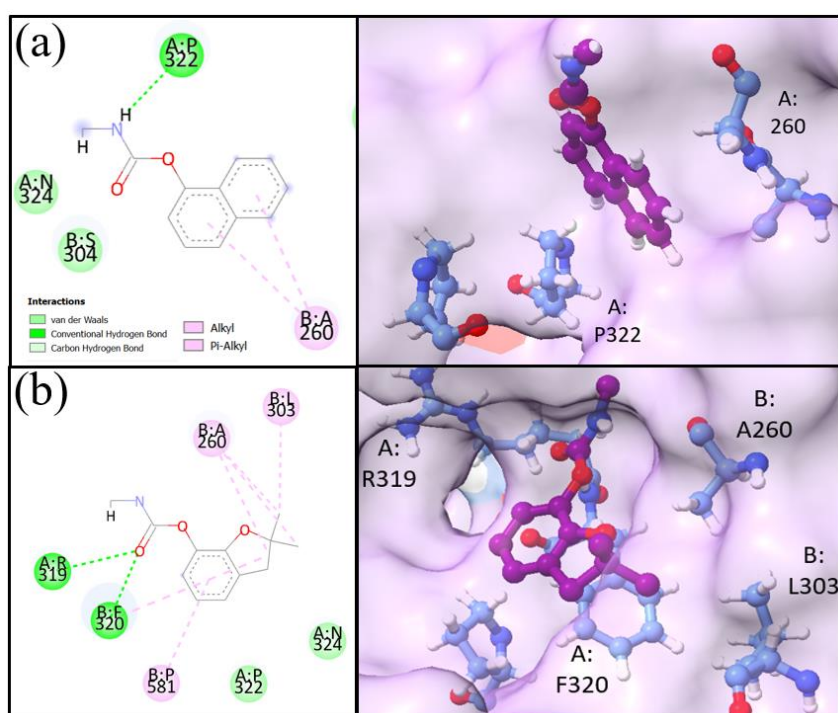


Figure 8. 2D interaction diagram of (a) carbaryl and (b) carbofuran depicting hydrogen bonds and alkyl interactions in the pocket

4. Conclusions

Methyl parathion hydrolase enzyme is widely studied these days for their application in bioremediation. However, for the first time we studied the inhibition kinetics and its atomistic details with carbamates as potential inhibitors of the enzyme. Carbofuran and carbaryl are widely

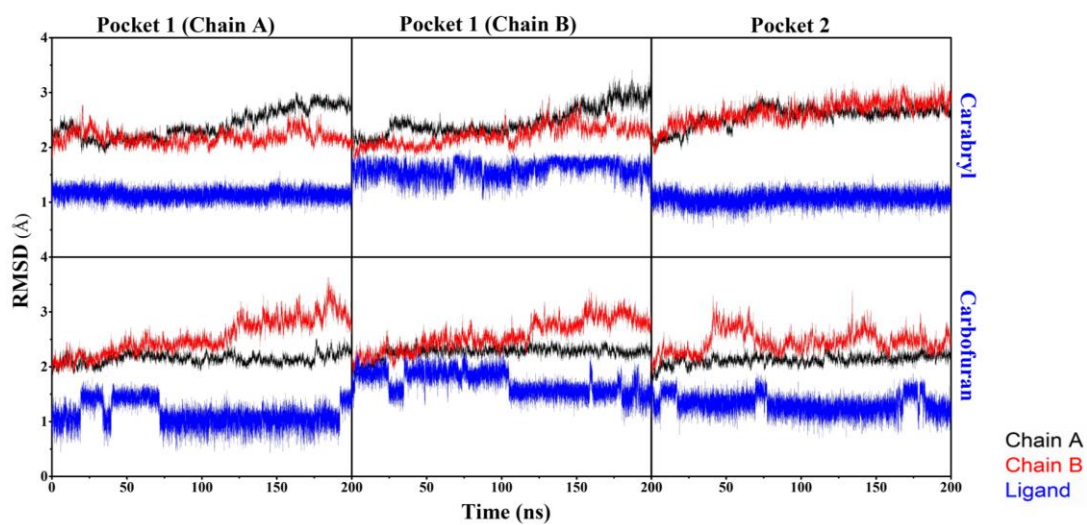
used carbamates in southeast Asian countries along with organophosphate pesticides. It was seen that inhibitor exhibited mixed type of inhibition. However, it must be noted the inhibition was significant only at high inhibitor concentration which is less likely to be present in the nature. This study provides fresh insights into the key residues involved in inhibitor binding. Combining the enzyme kinetics and molecular dynamic studies facilitates to understand the nature of enzyme inhibition which would help in the better application of this enzyme for bioremediation.

Conflict of interest

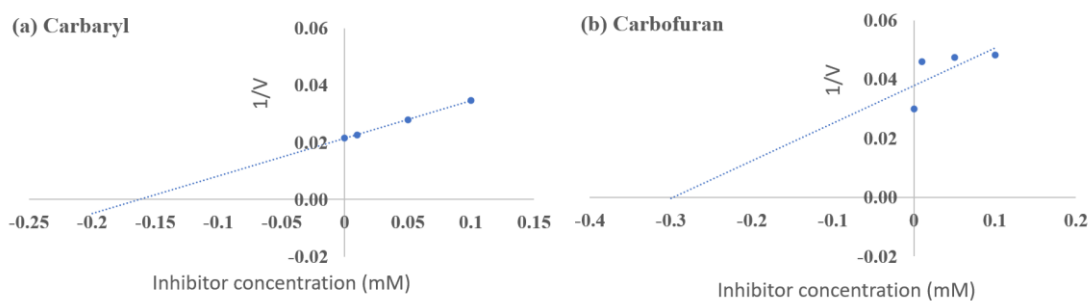
The authors have declared that these are no conflict of interest.

Acknowledgement

This work was financially supported by the Thailand Research Fund (grant number SA6280085). N.B. thanks the 90th Anniversary of Chulalongkorn University Fund (Ratchadaphiseksomphot Endowment Fund).



Supplementary figure 1. RMSD of chain A (red) chain B (black) and the carbamate (blue) for 100 ns in different binding pockets



Supplementary figure 2. Dixon plots of (a) carbaryl and (b) carbofuran

CONCLUSIONS

3.1 Conclusions

The aim of this work was to study and understand the binding mechanisms of two organophosphate hydrolases with various OP pesticides. Computational methods were explored to gain mechanistic insights of substrate binding and subsequent changes in the active site of the enzyme. In part I, glycerophosphodiesterase (GpdQ) was studied to understand effect of pesticide binding (profenofos, chlorpyrifos and diazinon) on active site geometry. The coordination chemistry of the metal ions in particular the beta metal ion changed to accommodate the bulky pesticide. Which is concomitant with the mechanism of catalysis. The binding free energy (ΔG_{bind}) of profenofos, diazinon and chlorpyrifos suggested good binding of the pesticides to the active site of the enzyme thus implying good catalysis. In part II, the binding mechanism of two different pesticides (profenofos and dichlorvos) towards methyl parathion hydrolase was explored and was compared with its natural substrate methyl paraxon. The promiscuity of the enzyme was also analyzed with two metal ions i.e., Cobalt and Zinc. It was seen that the pesticides coordinated with alpha metal ion of the enzyme. Both pesticides showed stronger binding in comparison to methyl paraxon. However, it was seen that the cobalt bound MPH had better substrate binding in comparison to zinc bound MPH. In the final part, the synergism of the MPH enzyme was analyzed with carbamate pesticides. Binding pocket analysis revealed three different binding pockets apart from the active site of the enzyme. All the binding pockets were exploited by molecular dynamics simulations. To validate kinetic studies was carried

spectroscopically with methyl paraxon (0.2 – 0.8 mM) as substrate and in presence (0.05 – 0.1 mM) and absence of carbamates (carbaryl and carbofuran) as inhibitor. Results revealed uncompetitive inhibition at high inhibitor concentrations only. To sum up, these enzymes have evolved to degrade toxic man-made compounds and thus understanding these enzymes in molecular level would help in evolving these in mechanistic context.

3.2 Suggestion for future study

1. Mutational studies at the inhibitor binding site could be carried out to know the residues that could contribute to enzyme inhibition.
2. The knowledge obtained here could have a potential value in designing of environmentally friendly bioremediation agents.

REFERENCES

1. Pope, C. N., Organophosphorus pesticides: DO they all have the same mechanism of toxicity? *Journal of Toxicology and Environmental Health, Part B* **1999**, 2 (2), 161-181.
2. Costa, L. G., Current issues in organophosphate toxicology. *Clinica chimica acta* **2006**, 366 (1-2), 1-13.
3. Singh, B. K.; Walker, A., Microbial degradation of organophosphorus compounds. *FEMS microbiology reviews* **2006**, 30 (3), 428-471.
4. Falahati-Pour, S. K.; Lotfi, A. S.; Ahmadian, G.; Baghizadeh, A.; Behroozi, R.; Haghghi, F., High-level extracellular secretion of organophosphorous hydrolase of *Flavobacterium* sp. in *Escherichia coli* BL21 (DE3) pLysS. *Biotechnology and applied biochemistry* **2016**, 63 (6), 870-876.
5. Edwards, F.; Tchounwou, P., Environmental toxicology and health effects associated with methyl parathion exposure—a scientific review. *International Journal of Environmental Research and Public Health* **2005**, 2 (3), 430-441.
6. Yang, C.; Cai, N.; Dong, M.; Jiang, H.; Li, J.; Qiao, C.; Mulchandani, A.; Chen, W., Surface display of MPH on *Pseudomonas putida* JS444 using ice nucleation protein and its application in detoxification of organophosphates. *Biotechnology and bioengineering* **2008**, 99 (1), 30-37.
7. Sethunathan, N.; Yoshida, T., A *Flavobacterium* sp. that degrades diazinon and parathion. *Canadian Journal of Microbiology* **1973**, 19 (7), 873-875.
8. Munnecke, D. M., Enzymatic hydrolysis of organophosphate insecticides, a possible pesticide disposal method. *Applied and Environmental Microbiology* **1976**, 32 (1), 7-13.
9. Serdar, C. M.; Gibson, D. T.; Munnecke, D. M.; Lancaster, J. H., Plasmid Involvement in Parathion Hydrolysis by *Pseudomonas diminuta*. *Applied and environmental microbiology* **1982**, 44 (1), 246-249.
10. Mulbry, W. W.; Karns, J. S.; Kearney, P. C.; Nelson, J. O.; McDaniel, C. S.; Wild, J. R., Identification of a plasmid-borne parathion hydrolase gene from *Flavobacterium* sp. by southern hybridization with opd from *Pseudomonas diminuta*. *Applied and environmental microbiology* **1986**, 51 (5), 926-930.

11. Harper, L. L.; McDaniel, C. S.; Miller, C. E.; Wild, J. R., Dissimilar plasmids isolated from *Pseudomonas diminuta* MG and a *Flavobacterium* sp. (ATCC 27551) contain identical *opd* genes. *Applied and environmental microbiology* **1988**, *54* (10), 2586-2589.
12. Horne, I.; Sutherland, T. D.; Harcourt, R. L.; Russell, R. J.; Oakeshott, J. G., Identification of an *opd* (organophosphate degradation) gene in an *Agrobacterium* isolate. *Applied and environmental microbiology* **2002**, *68* (7), 3371-3376.
13. Horne, I.; Qiu, X.; Russell, R. J.; Oakeshott, J. G., The phosphotriesterase gene *opdA* in *Agrobacterium radiobacter* P230 is transposable. *FEMS Microbiology Letters* **2003**, *222* (1), 1-8.
14. Primo-Parmo, S. L.; Sorenson Rc Fau - Teiber, J.; Teiber J Fau - La Du, B. N.; La Du, B. N., The human serum paraoxonase/arylesterase gene (PON1) is one member of a multigene family. (0888-7543 (Print)).
15. Eckerson, H. W.; Wyte, C. M.; La Du, B. N., The human serum paraoxonase/arylesterase polymorphism. *Am J Hum Genet* **1983**, *35* (6), 1126-1138.
16. Draganov, D., Lactonases with organophosphatase activity: Structural and evolutionary perspectives. *Chemico-biological interactions* **2010**, *187*, 370-2.
17. Zhongli, C.; Shunpeng, L.; Guoping, F., Isolation of methyl parathion-degrading strain M6 and cloning of the methyl parathion hydrolase gene. *Applied and environmental microbiology* **2001**, *67* (10), 4922-4925.
18. Fu, G.; Cui Z Fau - Huang, T.; Huang T Fau - Li, S.; Li, S., Expression, purification, and characterization of a novel methyl parathion hydrolase. (1046-5928 (Print)).
19. Liu, H.; Zhang, J.-J.; Wang, S.-J.; Zhang, X.-E.; Zhou, N.-Y., Plasmid-borne catabolism of methyl parathion and p-nitrophenol in *Pseudomonas* sp. strain WBC-3. *Biochemical and Biophysical Research Communications* **2005**, *334* (4), 1107-1114.
20. Zhang, R.; Cui Z Fau - Zhang, X.; Zhang X Fau - Jiang, J.; Jiang J Fau - Gu, J.-D.; Gu Jd Fau - Li, S.; Li, S., Cloning of the organophosphorus pesticide hydrolase gene clusters of seven degradative bacteria isolated from a methyl parathion contaminated site and evidence of their horizontal gene transfer. (0923-9820 (Print)).
21. Scharff, E. I.; Koepke J Fau - Fritsch, G.; Fritsch G Fau - Lücke, C.; Lücke C Fau - Rüterjans, H.; Rüterjans, H., Crystal structure of diisopropylfluorophosphatase from *Loligo vulgaris*. (0969-2126 (Print)).

22. Hoskin, F. C. G., Diisopropylphosphorofluoridate and Tabun: Enzymatic Hydrolysis and Nerve Function. *Science* **1971**, *172* (3989), 1243.
23. DeFrank, J. J.; Cheng, T. C., Purification and properties of an organophosphorus acid anhydrase from a halophilic bacterial isolate. (0021-9193 (Print)).
24. Cheng, T. C.; Harvey, S. P.; Chen, G. L., Cloning and expression of a gene encoding a bacterial enzyme for decontamination of organophosphorus nerve agents and nucleotide sequence of the enzyme. *Applied and environmental microbiology* **1996**, *62* (5), 1636-1641.
25. Daumann, L. J.; McCarthy, B. Y.; Hadler, K. S.; Murray, T. P.; Gahan, L. R.; Larrabee, J. A.; Ollis, D. L.; Schenk, G., Promiscuity comes at a price: catalytic versatility vs efficiency in different metal ion derivatives of the potential bioremediator GpdQ. *Biochimica et Biophysica Acta (BBA) - Proteins and Proteomics* **2013**, *1834* (1), 425–432.
26. Hadler, K. S.; Mitić, N.; Ely, F.; Hanson, G. R.; Gahan, L. R.; Larrabee, J. A.; Ollis, D. L.; Schenk, G., Structural flexibility enhances the reactivity of the bioremediator glycerophosphodiesterase by fine-tuning its mechanism of hydrolysis. *Journal of the American Chemical Society* **2009**, *131* (33), 11900–11908.
27. Hadler, K. S.; Tanifum, E. A.; Yip, S. H.; Mitić, N.; Guddat, L. W.; Jackson, C. J.; Gahan, L. R.; Nguyen, K.; Carr, P. D.; Ollis, D. L.; Hengge, A. C.; Larrabee, J. A.; Schenk, G., Substrate-promoted formation of a catalytically competent binuclear center and regulation of reactivity in a glycerophosphodiesterase from *Enterobacter aerogenes*. *Journal of the American Chemical Society* **2008**, *130* (43), 14129–14138.
28. Jackson, C. J.; Hadler, K. S.; Carr, P. D.; Oakley, A. J.; Yip, S.; Schenk, G.; Ollis, D. L., Malonate- bound structure of the glycerophosphodiesterase from *Enterobacter aerogenes* (GpdQ) and characterization of the native Fe²⁺ metal-ion preference. *Acta Crystallographica Section F: Structural Biology Communications* **2008**, *64* (8), 681–685.
29. Mirams, R. E.; Smith, S. J.; Hadler, K. S.; Ollis, D. L.; Schenk, G.; Gahan, L. R., Cadmium(II) complexes of the glycerophosphodiester- degrading enzyme GPDQ and a biomimetic N, O ligand. *Journal Biological Inorganic Chemistry* **2008**, *13* (7), 1065–1072.
30. Merone, L.; Mandrich L Fau - Rossi, M.; Rossi M Fau - Manco, G.; Manco, G., A thermostable phosphotriesterase from the archaeon *Sulfolobus solfataricus*: cloning, overexpression and properties. (1431-0651 (Print)).

31. Afriat, L.; Roodveldt, C.; Manco, G.; Tawfik, D. S., The Latent Promiscuity of Newly Identified Microbial Lactonases Is Linked to a Recently Diverged Phosphotriesterase. *Biochemistry* **2006**, *45* (46), 13677-13686.
32. Porzio, E.; Merone, L.; Mandrich, L.; Rossi, M.; Manco, G., A new phosphotriesterase from *Sulfolobus acidocaldarius* and its comparison with the homologue from *Sulfolobus solfataricus*. *Biochimie* **2007**, *89* (5), 625-636.
33. Hawwa, R.; Aikens, J.; Turner, R. J.; Santarsiero, B. D.; Mesecar, A. D., Structural basis for thermostability revealed through the identification and characterization of a highly thermostable phosphotriesterase-like lactonase from *Geobacillus stearothermophilus*. *Arch Biochem Biophys* **2009**, *488* (2), 109-120.
34. Chow, J. Y.; Xue B Fau - Lee, K. H.; Lee Kh Fau - Tung, A.; Tung A Fau - Wu, L.; Wu L Fau - Robinson, R. C.; Robinson Rc Fau - Yew, W. S.; Yew, W. S., Directed evolution of a thermostable quorum-quenching lactonase from the amidohydrolase superfamily. (1083-351X (Electronic)).
35. Hiblot, J.; Gotthard, G.; Chabriere, E.; Elias, M., Structural and Enzymatic characterization of the lactonase SisLac from *Sulfolobus islandicus*. *PLOS ONE* **2012**, *7* (10), e47028.
36. Kallnik, V.; Bunescu, A.; Sayer, C.; Bräsen, C.; Wohlgemuth, R.; Littlechild, J.; Siebers, B., Characterization of a phosphotriesterase-like lactonase from the hyperthermoacidophilic crenarchaeon *Vulcanisaeta moutnovskia*. *Journal of Biotechnology* **2014**, *190*, 11-17.
37. Yang, C.; Liu N Fau - Guo, X.; Guo X Fau - Qiao, C.; Qiao, C., Cloning of mpd gene from a chlorpyrifos-degrading bacterium and use of this strain in bioremediation of contaminated soil. (0378-1097 (Print)).
38. Zhang, R.; Cui Z Fau - Jiang, J.; Jiang J Fau - He, J.; He J Fau - Gu, X.; Gu X Fau - Li, S.; Li, S., Diversity of organophosphorus pesticide-degrading bacteria in a polluted soil and conservation of their organophosphorus hydrolase genes. (0008-4166 (Print)).
39. Ely, F.; Foo, J.-L.; Jackson, C. J.; Gahan, L. R.; Ollis, D.; Schenk, G., Enzymatic bioremediation: Organophosphate degradation by binuclear metallo-hydrolases. *Current Topics in Biochemical Research* **2007**, *9* (2), 63-78.
40. Mitić, N.; Smith, S. J.; Neves, A.; Guddat, L. W.; Gahan, L. R.; Schenk, G., The catalytic mechanisms of binuclear metallohydrolases. *Chemical Reviews* **2006**, *106* (8), 3338–3363.

41. Larson, T. J.; Ehrmann, M.; Boos, W., Periplasmic glycerophosphodiester phosphodiesterase of *Escherichia coli*, a new enzyme of the glp regulon. *Journal of Biological Chemistry* **1983**, *258* (9), 5428–5432.
42. Gerlt, J. A.; Westheimer, F. H., Phosphodiesterase from *Enterobacter Aerogenes*. *Journal of the American Chemical Society* **1973**, *95* (24), 8166–8168.
43. Gerlt, J. A.; Whitman, G. J., Purification and properties of a phosphohydrolase from *Enterobacter Aerogenes*. *Journal of Biological Chemistry* **1975**, *250* (13), 5053–5058.
44. Ghanem, E.; Li, Y.; Xu, C.; Raushel, F. M., Characterization of a phosphodiesterase capable of hydrolyzing EA 2192, the most toxic degradation product of the nerve agent VX. *Biochemistry* **2007**, *46* (31), 9032–9040.
45. Schenk, G.; Mateen, I.; Ng, T.-K.; Pedroso, M. M.; Mitic, N.; Jafelicci, M.; Marques, R. F. C.; Gahan, L. R.; Ollis, D. L., Organophosphate-degrading metallohydrolases: Structure and function of potent catalysts for applications in bioremediation. *Coordination Chemistry Reviews* **2016**, *317*, 122–131.
46. Ghanem, E.; Raushel, F., Detoxification of organophosphate nerve agents by bacterial phosphotriesterase. *Toxicology and Applied Pharmacology* **2005**, *207* (2), 459–470.
47. Wilcox, D. E., Binuclear Metallohydrolases. *Chem. Rev.* **1996**, *96*, 2435–2458.
48. Jackson, C. J.; Carr, P. D.; Liu, J.-W.; Watt, S. J.; Beck, J. L.; Ollis, D. L., The structure and function of a novel glycerophosphodiesterase from *Enterobacter Aerogenes*. *Journal of Molecular Biology* **2007**, *367* (4), 1047–1062.
49. Pedroso, M. M.; Ely, F.; Carpenter, M. C.; Mitic, N.; Gahan, L. R.; Ollis, D. L.; Wilcox, D. E.; Schenk, G., Mechanistic insight from calorimetric measurements of the assembly of the binuclear metal active site of glycerophosphodiesterase (GpdQ) from *Enterobacter Aerogenes*. *Biochemistry* **2017**, *56* (26), 3328–3336.
50. Sharma, G.; Jayasinghe-Arachchige, V. M.; Hu, Q.; Schenk, G.; Prabhakar, R., Effect of Chemically Distinct Substrates on the Mechanism and Reactivity of a Highly Promiscuous Metallohydrolase. *ACS Catalysis* **2020**, *10* (6), 3684–3696.
51. Aktar, W.; Sengupta, D.; Chowdhury, A., Impact of pesticides use in agriculture: their benefits and hazards. *Interdisciplinary Toxicology* **2009**, *2* (1), 1–12.
52. Abou-Donia, M. B., Organophosphorus Ester-Induced Chronic Neurotoxicity. *Archives of*

Environmental Health: An International Journal **2003**, 58 (8), 484-497.

53. Ragnarsdottir, K. V., Environmental fate and toxicology of organophosphate pesticides. *Journal of the Geological Society* **2000**, 157 (4), 859-876.

54. Berman, T.; Barnett-Itzhaki, Z.; Göen, T.; Hamama, Z.; Axelrod, R.; Keinan-Boker, L.; Shimony, T.; Goldsmith, R., Organophosphate pesticide exposure in children in Israel: Dietary associations and implications for risk assessment. *Environmental Research* **2020**, 182, 108739.

55. Perez-Fernandez, C.; Morales-Navas, M.; Aguilera-Sáez, L. M.; Abreu, A. C.; Guardia-Escote, L.; Fernández, I.; Garrido-Cárdenas, J. A.; Colomina, M. T.; Giménez, E.; Sánchez-Santed, F., Medium and long-term effects of low doses of Chlorpyrifos during the postnatal, preweaning developmental stage on sociability, dominance, gut microbiota and plasma metabolites. *Environmental Research* **2020**, 184, 109341.

56. Richins, R. D.; Kaneva, I.; Mulchandani, A.; Chen, W., Biodegradation of organophosphorus pesticides by surface-expressed organophosphorus hydrolase. *Nature Biotechnology* **1997**, 15, 984-987.

57. Schenk, G.; Mateen, I.; Ng, T.-K.; Pedroso, M.; Mitić, N.; Miguel, J.; Marques, R.; Gahan, L.; Ollis, D., Organophosphate-degrading metallohydrolases: Structure and function of potent catalyst for applications in bioremediation. *Coordination Chemistry Reviews* **2016**, 317.

58. Mazur, A., An enzyme in animal tissues capable of hydrolysing the phosphorus-fluorine bond of alkyl fluorophosphates. *Journal of Biological Chemistry* **1946**, 164, 271-289.

59. Ratna Kumari, A.; Sobha, K.; Mounika, K.; Nageswara Rao, G. J.; Ashok, M., Molecular characterization of bacteria capable of organophosphate degradation. *International Journal of Life Sciences Biotechnology and Pharma Research* **2012**, 1 (3), 64-70.

60. Brooks, B. R.; Bruccoleri, R. E.; Olafson, B. D.; States, D. J.; Swaminathan, S.; Karplus, M., CHARMM: A program for macromolecular energy minimization and dynamics calculations. *Journal of Computational Chemistry* **1983**, 4 (2), 187-217.

61. Olsson, M. H.; Sondergaard, C. R.; Rostkowski, M.; Jensen, J. H., PROPKA3: Consistent treatment of internal and surface residues in empirical pKa predictions. *Journal of Chemical Theory and Computation* **2011**, 7 (2), 525-537.

62. Maier, J. A.; Martinez, C.; Kasavajhala, K.; Wickstrom, L.; Hauser, K. E.; Simmerling, C., ff14SB: Improving the Accuracy of Protein Side Chain and Backbone Parameters from ff99SB. *Journal of Chemical Theory and Computation* **2015**, *11* (8), 3696-3713.
63. Frisch, M. J.; Trucks, G. W.; Schlegel, H. B.; Scuseria, G. E.; Robb, M. A.; Cheeseman, J. R.; Scalmani, G.; Barone, V.; Mennucci, B.; Petersson, G. A.; Nakatsuji, H.; Caricato, M.; Li, X.; Hratchian, H. P.; Izmaylov, A. F.; Bloino, J.; Zheng, G.; Sonnenberg, J. L.; Hada, M.; Ehara, M.; Toyota, K.; Fukuda, R.; Hasegawa, J.; Ishida, M.; Nakajima, T.; Honda, Y.; O.Kitao; Nakai, H.; Vreven, T.; Jr., J. A. M.; Peralta, J. E.; Ogliaro, F.; M.J.Bearpark; Heyd, J.; Brothers, E. N.; Kudin, K. N.; Staroverov, V. N.; Kobayashi, R.; J.Normand; Raghavachari, K.; Rendell, A. P.; Burant, J. C.; Iyengar, S. S.; Tomasi, J.; M.Cossi; Rega, N.; Millam, N. J.; Klene, M.; Knox, J. E.; Cross, J. B.; Bakken, V.; Adamo, C.; J.Jaramillo; Gomperts, R.; Stratmann, R. E.; Yazyev, O.; Austin, A. J.; Cammi, R.; Pomelli, C.; Ochterski, J. W.; Martin, R. L.; Morokuma, K.; Zakrzewski, V. G.; Voth, G. A.; Salvador, P.; Dannenberg, J. J.; Dapprich, S.; Daniels, A. D.; Farkas, Ö.; Foresman, J. B.; Ortiz, J. V.; J.Cioslowski; Fox, D. J., Gaussian 09. Wallingford, CT: Gaussian. **2009**.
64. Wang, J.; Wolf, R. M.; Caldwell, J. W.; Kollman, P. A.; Case, D. A., Development and testing of a general amber force field. *Journal of Computational Chemistry* **2004**, *25* (9), 1157-1174.
65. Srinivas, K. V. N. S.; Rao, Y. K.; Mahendar, I.; Biswanth, D.; Ramakrishna, K. V. S.; Kishore, K. H.; Murty, U. S. N., Flavanoids from *Caesalpinia pulcherrima*. *Phytochemistry* **2003**, *63*, 789-793.
66. Price, D. J.; Brooks, C. L., A modified TIP3P water potential for simulation with Ewald summation. *Journal of Chemical Physics* **2004**, *121* (20), 10096-10103.
67. York, D. M.; Darden, T. A.; Pedersen, L. G., The effect of long-range electrostatic interactions in simulations of macromolecular crystals: A comparison of the Ewald and truncated list methods. *The Journal of Chemical Physics* *99*(10) **1993**, 8345-8348.
68. Ryckaert, J.-P.; Ciccotti, G.; Berendsen, H. J. C., Numerical integration of the Cartesian equations of motion of a system with constraints: molecular dynamics of n-alkanes. *Journal of Computational Physics* **1977**, *23* (3), 327-341.
69. Uberuaga, B. P.; Anghel, M.; Voter, A. F., Synchronization of trajectories in canonical molecular-dynamics simulations: Observation, explanation, and exploitation. *Journal of Chemical Physics* **2004**, *120* (14), 6363-6374.

70. Berendsen, H. J. C.; Postma, J. P. M.; Gunsteren, W. F. v.; DiNola, A.; Haak, J. R., Molecular dynamics with coupling to an external bath. *Journal of Chemical Physics* **1984**, *81* (8), 3684–3690.
71. Case, D. A.; Betz, R. M.; Cerutti, D. S.; III, T. E. C.; Darden, T. A.; Duke, R. E.; Giese, T. J.; Gohlke, H.; Goetz, A. W.; Homeyer, N.; Izadi, S.; Janowski, P.; Kaus, J.; Kovalenko, A.; Lee, T. S.; LeGrand, S.; Li, P.; C.Lin; Luchko, T.; Luo, R.; Madej, B.; Mermelstein, D.; Merz, K. M.; Monard, G.; Nguyen, H.; Nguyen, H. T.; Omelyan, I.; Onufriev, A.; Roe, D. R.; Roitberg, A.; Sagui, C.; Simmerling, C. L.; Botello-Smith, W. M.; J. Swails; Walker, R. C.; Wang, J.; Wolf, R. M.; Wu, X.; Xiao, L.; Kollman, P. A., *Amber 2016*. University of California, Sanfrancisco, 2016.
72. Roe, D. R.; Cheatham, T. E., PTRAJ and CPPTRAJ: Software for processing and analysis of molecular dynamics trajectory data. *Journal of Chemical Theory and Computation* **2013**, *9* (7), 3084-3095.
73. Genheden, S.; Ryde, U., The MM/PBSA and MM/GBSA methods to estimate ligand-binding affinities. *Expert Opinion on Drug Discovery* **2015**, *10* (5), 449-461.
74. Kollman, P. A.; Massova, I.; Reyes, C.; Kuhn, B.; Huo, S.; Chong, L.; Lee, M.; Lee, T.; Duan, Y.; Wang, W.; Donini, O.; Cieplak, P.; Srinivasan, J.; Case, D. A.; Cheatham, T. E., Calculating structures and free energies of complex molecules: combining molecular mechanics and continuum models. *Accounts of Chemical Research* **2000**, *33* (12), 889-897.
75. Kollman, P. A.; Massova, I.; Reyes, C.; Kuhn, B.; Huo, S.; Chong, L.; Lee, M.; Lee, T.; Duan, Y.; Wang, W.; Donini, O.; Cieplak, P.; Srinivasan, J.; Case, D. A.; Cheatham, T. E., 3rd, Calculating structures and free energies of complex molecules: combining molecular mechanics and continuum models. *Accounts of chemical research* **2000**, *33* (12), 889-97.
76. Sitkoff, D.; Sharp, K. A.; Honig, B., Accurate Calculation of Hydration Free Energies Using Macroscopic Solvent Models. *The Journal of Physical Chemistry* **1994**, *98*(7), 1978-1988.
77. Sharma, G.; Hu, Q.; Jayasinghe-Arachchige, V. M.; Paul, T. J.; Schenk, G.; Prabhakar, R., Investigating coordination flexibility of glycerophosphodiesterase (GpdQ) through interactions with mono-, di-, and triphosphoester (NPP, BNPP, GPE, and paraoxon) substrates. *Phys.Chem.Chem.Phys.*, **2019**, *21*, 5499.
78. Paul, T. J.; Schenk, G.; Prabhakar, R., Formation of catalytically active binuclear center of glycerophosphodiesterase: A molecular dynamics study. *The Journal of Physical Chemistry B* **2018**,

122 (22), 5797–5808.

79. Sharma, G.; Hu, Q.; Jayasinghe-Arachchige, V. M.; Paul, T. J.; Schenk, G.; Prabhakar, R., Investigating coordination flexibility of glycerophosphodiesterase (GpdQ) through interactions with mono-, di-, and triphosphoester (NPP, BNPP, GPE, and paraoxon) substrates. *Physical Chemistry Chemical Physics* **2019**, *21* (10), 5499-5509.
80. Tidor, B.; Karplus, M., The contribution of vibrational entropy to molecular association: The dimerization of insulin. *Journal of Molecular Biology* **1994**, *238* (3), 405-414.
81. Adeyinka, A.; Muco, E.; Pierre, L., Organophosphates. BTI - StatPearls.
82. Da Silva, N. A.; Birolli, W. G.; Seleglim, M. H. R.; Porto, A. L. M., Biodegradation of the organophosphate pesticide profenofos by marine fungi. In *Applied Bioremediation-Active and Passive Approaches*, IntechOpen: 2013.
83. Chu, X.; Zhang X Fau - Chen, Y.; Chen Y Fau - Liu, H.; Liu H Fau - Song, D.; Song, D., [Study on the properties of methyl parathion hydrolase from *Pseudomonas* sp. WBC-3]. (0001-6209 (Print)).
84. Sun, L.; Dong Y Fau - Zhou, Y.; Zhou Y Fau - Yang, M.; Yang M Fau - Zhang, C.; Zhang C Fau - Rao, Z.; Rao Z Fau - Zhang, X.-e.; Zhang, X. E., Crystallization and preliminary X-ray studies of methyl parathion hydrolase from *Pseudomonas* sp. WBC-3. (0907-4449 (Print)).
85. Ng, T.-K.; Gahan, L. R.; Schenk, G.; Ollis, D. L., Altering the substrate specificity of methyl parathion hydrolase with directed evolution. *Arch Biochem Biophys* **2015**, *573*, 59-68.
86. Purg, M.; Pabis, A.; Baier, F.; Tokuriki, N.; Jackson, C.; Kamerlin, S. A.-O., Probing the mechanisms for the selectivity and promiscuity of methyl parathion hydrolase. LID - 20160150. (1364-503X (Print)).
87. Boratyn, G. M.; Camacho, C.; Cooper, P. S.; Coulouris, G.; Fong, A.; Ma, N.; Madden, T. L.; Matten, W. T.; McGinnis, S. D.; Merezuk, Y.; Raytselis, Y.; Sayers, E. W.; Tao, T.; Ye, J.; Zaretskaya, I., BLAST: a more efficient report with usability improvements. *Nucleic Acids Res* **2013**, *41* (Web Server issue), W29-W33.
88. Johnson, M.; Zaretskaya I Fau - Raytselis, Y.; Raytselis Y Fau - Merezuk, Y.; Merezuk Y Fau - McGinnis, S.; McGinnis S Fau - Madden, T. L.; Madden, T. L., NCBI BLAST: a better web interface. (1362-4962 (Electronic)).
89. Ely, F.; Foo, J.; Jackson, C.; Gahan, L.; Ollis, D.; Schenk, G., Enzymatic bioremediation:

- Organophosphate degradation by binuclear metallo-hydrolases. *Curr. Top. Biochem. Res.* **2011**, *9*.
90. Bigley, A. N.; Raushel, F. M., Catalytic mechanisms for phosphotriesterases. (0006-3002 (Print)).
91. Rani, N. L.; Lalithakumari, D., Degradation of methyl parathion by *Pseudomonas putida*. (0008-4166 (Print)).
92. Singh, B. K., Organophosphorus-degrading bacteria: ecology and industrial applications. *Nature Reviews Microbiology* **2009**, *7* (2), 156-164.
93. Ufarté, L.; Laville, E.; Duquesne, S.; Morgavi, D.; Robe, P.; Klopp, C.; Rizzo, A.; Pizzut-Serin, S.; Potocki-Veronese, G., Discovery of carbamate degrading enzymes by functional metagenomics. *PLOS ONE* **2017**, *12* (12), e0189201.
94. Wang, Q.; Lemley, A. T., Competitive Degradation and Detoxification of Carbamate Insecticides by Membrane Anodic Fenton Treatment. *Journal of Agricultural and Food Chemistry* **2003**, *51* (18), 5382-5390.
95. Farnoosh, G.; Latifi, A. M.; Khajeh, K.; Aghamollaei, H.; Najafi, A., Enzymatic degradation of organophosphate compounds: evaluation of high-level production, solubility and stability. *Journal of Applied Biotechnology Reports* **2015**, *2* (4), 343-48.
96. Yu, J.; Zhou, Y.; Tanaka, I.; Yao, M., Roll: a new algorithm for the detection of protein pockets and cavities with a rolling probe sphere. *Bioinformatics* **2010**, *26* (1), 46-52.
97. Gordon, J.; Myers, J.; Folta, T.; Shoja, V.; Heath, L.; Onufriev, A., H⁺⁺: A server for estimating pK_as and adding missing hydrogens to macromolecules. *Nucleic Acids Res* **2005**, *33*, W368-71.
98. Myers, J.; Grothaus, G.; Narayanan, S.; Onufriev, A., A simple clustering algorithm can be accurate enough for use in calculations of pK_s in macromolecules. *Proteins* **2006**, *63*, 928-38.
99. Rarey, M.; Kramer, B.; Lengauer, T.; Klebe, G., A Fast Flexible Docking Method using an Incremental Construction Algorithm. *Journal of Molecular Biology* **1996**, *261* (3), 470-489.



จุฬาลงกรณ์มหาวิทยาลัย
CHULALONGKORN UNIVERSITY

VITA

NAME Nayana Bhat

DATE OF BIRTH 15 February 1988

PLACE OF BIRTH Manipal, Karnataka, India

INSTITUTIONS ATTENDED Bangalore University
Chulalongkorn University

HOME ADDRESS 60/134, Supalai Premier Place Asok, Asok Montri Rd, Khlong Toei Nuea,
Wattana, Bangkok 10110



จุฬาลงกรณ์มหาวิทยาลัย
CHULALONGKORN UNIVERSITY